



# Reindeer prey mobility and seasonal hunting strategies in the late Gravettian mammoth steppe

A. J. E. Pryor<sup>1</sup> · T. Nesnídalová<sup>1</sup> · P. Šída<sup>2</sup> · G. Lengyel<sup>3,4</sup> · C. D. Standish<sup>5</sup> · J. A. Milton<sup>5</sup> · M. J. Cooper<sup>5</sup> · B. Hambach<sup>5</sup> · J. Crowley<sup>6</sup> · J. Wilczyński<sup>7</sup>

Received: 30 November 2022 / Accepted: 19 June 2024  
© The Author(s) 2024

## Abstract

Reindeer are part of the faunal suite that dominated central Europe during the last glacial cycle. Their importance to Late Gravettian hunters as prey and a source of raw materials (hide, bone, antler) is well attested, however the context of Late Gravettian reindeer predation is lesser understood. This paper presents an investigation of human and reindeer predator-prey interactions at the Late Gravettian kill-butcher site of Lubná VI, Czech Republic. We reconstruct seasonal mobility ( $^{87}\text{Sr}/^{86}\text{Sr}$ ,  $\delta^{18}\text{O}$ ), diet ( $\delta^{13}\text{C}$ ,  $\delta^{15}\text{N}$ ) and season of death (dental cementum) of up to nine reindeer prey, to inform on the strategic choices made by Late Gravettian hunters. Results indicate that most hunted reindeer lived year-round in the foothills of the Bohemian-Moravian highlands near where Lubná is located, at altitudes between ~200–450 m above present sea level, while a smaller number showed evidence of seasonal migration between this area and the open plains of the Elbe river corridor (Bohemian Cretaceous basin). No evidence for long distance migration of reindeer was detected, indicating that productive local environments were supporting reindeer herds within a single annual territory. Meanwhile, areas higher than ~450 m above present sea level were avoided entirely by all analysed individuals, consistent with these areas being topographic barriers to movement due to climate severity. We conclude that hunters visited Lubná as part of a logistically-organised subsistence strategy, deliberately targeting reindeer in late autumn when fat supplies, hides and antler are in prime condition knowing that they would reliably encounter their prey at this location.

**Keywords** Hunter-gatherer · Central Europe · Lubná · Strontium · Last glacial · Stable isotopes

## Introduction

The mammoth steppe is a no-analogue steppe-tundra ecosystem that covered extensive parts of central and eastern Europe during the last ice age (Guthrie 2001; Bocherens 2015). This unique ecology was characterised by high vegetative productivity comprising a rich herbaceous and grassland flora which supported diverse animal communities including megafauna, large and medium sized herbivores and numerous carnivorous species (Bråthen et al. 2021; Bocherens 2015; Schwartz-Narbonne et al. 2019). Climatic data indicate that after about 35,000 cal. years BP, and particularly during the Last Glacial Maximum (LGM, 26,500–19,000 cal. years BP; Clark et al. 2009), the mammoth steppe across much of central Europe was also an increasingly seasonal ecosystem with relatively short and warm summers contrasted by very cold winters with long-lasting snow cover and expansive permafrost across much of the region (Guthrie 2001; Denton et al. 2005; Ampel et al. 2010;

✉ A. J. E. Pryor  
Alex.Pryor@exeter.ac.uk

<sup>1</sup> Department of Archaeology and History, University of Exeter, Exeter, UK

<sup>2</sup> Institute of archaeology Czech Academy of Sciences, (Research Centre for the Paleolithic and Paleoanthropology), Brno, Czech Republic

<sup>3</sup> Hungarian National Museum (National Institute of Archaeology), Budapest, Hungary

<sup>4</sup> Department of Prehistory and Archaeology, University of Miskolc, Miskolc, Hungary

<sup>5</sup> School of Ocean & Earth Sciences, University of Southampton, Southampton, UK

<sup>6</sup> Unaffiliated Researcher, Exeter, UK

<sup>7</sup> Institute of Systematics and Evolution of Animals, Polish Academy of Sciences, Kraków, Poland

Lindgren et al. 2016). This combination of diverse fauna, enhanced climate seasonality and a mammoth steppe flora is thought to have stimulated seasonally-specific resource partitioning between fauna who were competing for food and habitat, including winter dietary specialisation during periods of food scarcity (Rivals et al. 2010; Schwartz-Narbonne et al. 2019), and possibly requiring a degree of seasonal mobility for at least some species.

For Late Gravettian hunter-gatherers living in Central Europe ~30,000–26,000 cal. years BP (Lengyel and Wilczyński 2018; Wilczyński et al. 2020), understanding the ecology and behaviour of mammoth steppe fauna and their response to seasonal changes in climate would have been critical to survival. Key prey species included mammoth, horse, reindeer, fox, wolf and hare, the remains of which are commonly found at Late Gravettian sites throughout the region (Brugère and Fontana 2009; Šída 2009a; Lipecki and Wojtal 1998; Wilczyński et al. 2012, 2015, 2021). These species were an important source of food, as well as a range of other raw materials including hide, bone (source of fat, raw material and/or fuel) and antler — all of which vary in quality or availability throughout the year (e.g. Speth and Spielman 1983; Stenton 1991; Pryor 2008). Late Gravettian hunter-gatherers would have needed to plan ahead to gain access to these resources at both the optimal time of year and at a point when the animal prey were physically available within reasonable geographic distances to where the hunters lived.

Recent analysis of the Late Gravettian reindeer kill-butcher site of Lubná VI, located in Bohemia, Czechia (~27,300 cal. years BP), has suggested that the Late Gravettian population of Central Europe was highly mobile (Wilczyński et al. 2021). This is indicated by a lithic assemblage composed entirely of raw materials originating outside of Bohemia, while the few lithic cores and high number of burins and backed lithic artefacts showed that hunting weaponry was primarily produced at the site from pre-manufactured blade blanks packed for travelling. As reindeer are known to migrate seasonally in some situations between summer and winter grounds (Bergman et al. 2000), the lithics data raise questions as to whether the apparently high mobility of the Late Gravettian population was forced upon them by highly mobile prey adapting to the increasingly severe climates of Central Europe one millennia prior to the onset of the LGM.

Here, we investigate this possibility through an intensive study of reindeer seasonal mobility and linked Late Gravettian hunting practices at Lubná VI using isotopic analysis of tooth enamel and the elements strontium, oxygen, carbon and nitrogen, in conjunction with dental cementum analysis. Our reconstructions of prey mobility reveal, for the first time, how reindeer adapted their mobility to the mammoth

steppe ecosystem in Central Europe, and increase understanding of the strategies developed by Late Gravettian hunters to survive during the last glacial period. The objectives were to:

1. Investigate seasonal mobility and diet of the reindeer prey targeted by Palaeolithic hunters at Lubná VI.
2. Establish season of death of the Lubná VI reindeer.
3. Reconstruct the hunting strategies of Late Gravettian hunters at Lubná VI by drawing inferences about choices they made due to the seasonal mobility of their prey.

## Lubná VI

The Lubná site complex is located in the western part of central Bohemia, Czechia, approximately 50 km west of Prague (50.08128°N; 13.70063°E), on a slight, southeast facing slope of the Na Pláni hill (Fig. 1). Since the 1890s, excavations and scattered finds have yielded a total of eight Upper Palaeolithic sites (Lubná I–VIII) across about 1,100 m of the landscape, which yielded bones, stone tools and fireplaces (Kušta 1891a, b; hm 1933; Vencl 1966; Šída 2009a, b, 2016), making it one of the richest Upper Palaeolithic site clusters in Bohemia. Lubná VI was discovered in 2006 (Šída 2009a, b), and a small trench (1m<sup>2</sup>) was excavated in 2012. This uncovered a fireplace surrounded by 162 lithics (including just 12 tools but many microchips) and a large number of bones (Šída 2016). A new phase of fieldwork conducted in 2018 excavated an additional area of 19 m<sup>2</sup> adjacent to the earlier trench, revealing two hearths, a stone pavement made of non-local manuport pebbles, numerous knapped lithic artefacts characteristic of a Late Gravettian industry and fauna consisting of at least seven reindeer and single specimens of Alpine ibex and woolly mammoth (Wilczyński et al. 2021). Radiocarbon dating of seven reindeer bones and one *Capra ibex* metatarsal places the site to between 27,500 and 27,100 cal. years BP (Wilczyński et al. 2020). Burins and backed implements dominate the tool inventory and the raw materials were brought a minimum distance of 120 km from either Lower Silesia in southwest Poland (Wilczyński et al. 2021), or Saxony (Šída 2016: 121). Zoological studies identified 3–5 month old reindeer in the assemblage indicating that the site was occupied in early autumn and functioned as a central camp to which whole carcasses were carried for hide removal and butchering (Wilczyński et al. 2021).

Lubná lies in the Tepla-Barrandian part of the Bohemian Massif, northwest of the Bohemian-Moravian Highlands that stretch northeasterly over 150 km between Bohemia

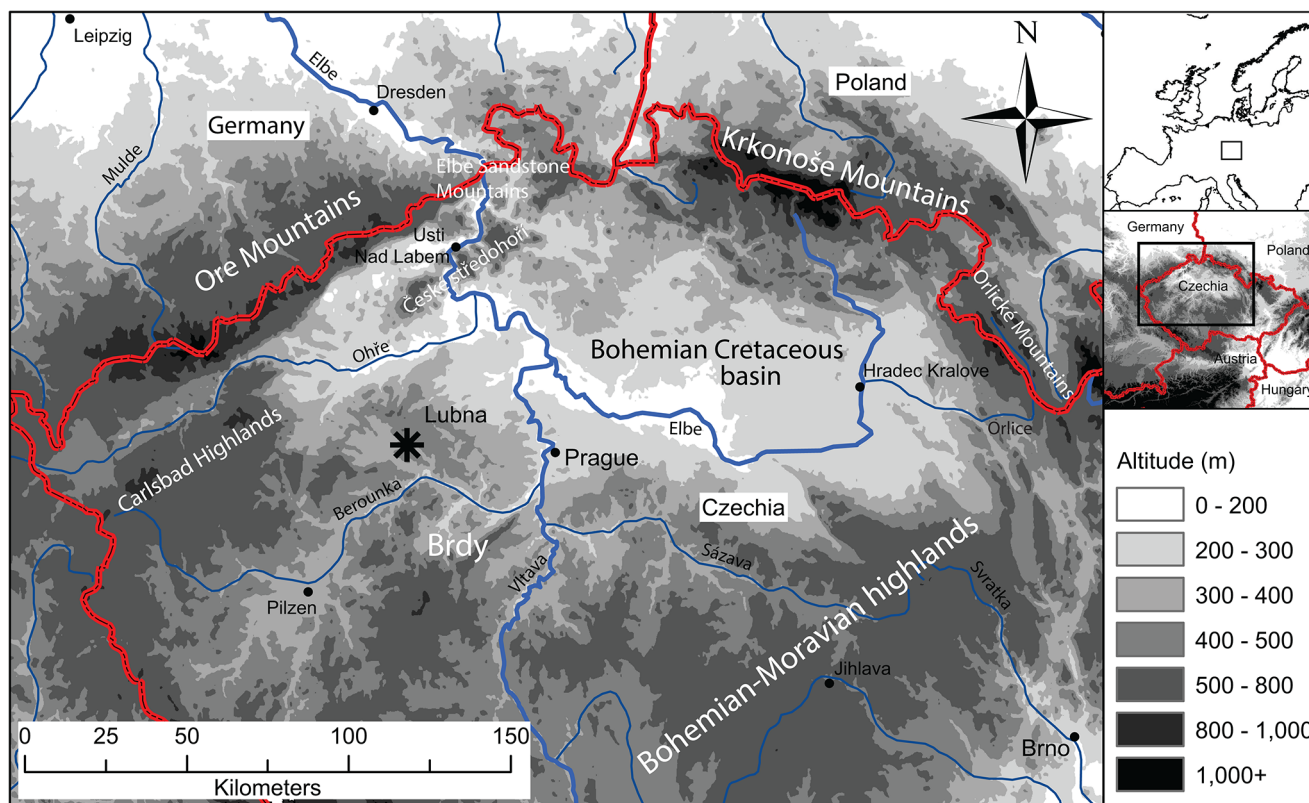


**Fig. 1** Topographic map showing Lubná VI and the surrounding physical context

and Moravia across the central part of Czechia. This large area of hills, rising up to 837 m above sea level, appears to have been mostly unoccupied by humans and large mammals in the Gravettian and Late Gravettian periods (Musil 2010; Škrdla et al. 2018; Verpoorte 2004) until it was recolonised in the Late Glacial (Škrdla et al. 2015). About 25 km northeast of Lubná the hills and valleys turn into the flatter, low-lying Bohemian Cretaceous Basin. On the other side of the basin is the highest part of the Bohemian Massif, the Sudetes, with the Krkonoše and Jizera Mountains in the northwest region, Orlické Mountains in the centre and the Jeseník Mountains in the southeast, terminating at the Moravian Gate and Ostrava basin. These higher mountains experienced small and localised glaciations during the LGM (Růžička 2004: 33) that had likely already started to form at the time Lubná was occupied and would have hindered movement at higher altitudes, channelling people and prey through the river corridors instead. West of the Sudetes lie the Elbe Sandstone Mountains through which the Elbe flows to Germany, creating a river valley corridor.

The nearest major river to Lubná, the Berounka, is approximately 12 km south of the site draining west to east into the river Vltava (Moldau), which flows northward meeting the river Elbe where the Bohemian Massif recedes into the Bohemian Basin. Approximately 20 km to the north, the river Ohře (Eger), a tributary to the river Elbe, originates

in Germany and flows between the Ore mountains and Carlsbad Highlands and drains into the Elbe before it enters Germany.

## Reindeer ecology

Today, semi-domesticated and wild reindeer have a northern circumpolar distribution at latitudinal extremes. Strictly sedentary and migratory ecotypes are known, however reindeer can also demonstrate “marked seasonal movement plasticity” (Theoret et al. 2022:12), being highly flexible in terms of mobility year-to-year at the scale of single individuals but also entire herds. Individual herds can occupy large ranges and, if migratory, may undertake seasonal movements over thousands of kilometres (Bergman et al. 2000). These movements can be related to thermal or dietary stress and usually occur on a north-south trajectory. Migrations over smaller distances are also common and are thought to be caused by factors such as forage abundance, insect pestilence and predation avoidance (Bergerud and Lutich 2003; Ferguson and Elkie 2004). The northerly spring migration typically happens between March and May and is led by pregnant females (Schaefer et al. 2000). The same calving areas are often used repeatedly (Skoog 1968), and birth normally occurs between late May and early June (Prichard et

al. 1999). After calving, the animals can disperse over wide areas and herds may fracture into smaller groups, with individuals from the same herd being hundreds of kilometres apart (Schaefer et al. 2000). These smaller groups aggregate again during the breeding season in late summer/early autumn, after which the southerly autumn migration begins, normally between mid-September to mid-November. This movement may be rapid, but it can also take several months (Parker 1972: 47). Reindeer diet consists mainly of grasses and shrubs in the summer (Bergerud 1972) and lichen in the winter (Boertje 1984). Calves are weaned at two to three months (Skoog 1968).

Reindeer tooth eruption intervals have been examined in various populations including Newfoundland caribou (Bergerud 1970), Barren-ground caribou, Kaminuriak, Nunavut (Miller 1974), Sisimut reindeer, Greenland (Pasda 2009), reindeer from Svalbard (van den Berg et al. 2020), and a Palaeolithic reindeer population from France (Bouchud 1966). The results are generally consistent, indicating that M1 typically erupts between 3 and 5 months, M2 between 7 and 15 months, M3 between 15 and 28 months and P4 between 12 and 30 months of age (Fig. 2), although variation between different subspecies and populations exists, likely due to genetic, dietary and environmental factors (van den Berg et al. 2021). Isotopic ratios in tooth enamel are fixed into the tissues at the point of mineralisation, and therefore reflect the period of tooth formation. Observed eruption intervals stretch over more than six months of the year in some elements, and can also vary by several months between different populations, especially in P4 and M3. This implies that mineralisation intervals could be equally variable, and thus the same tooth could record different parts of the year in different individuals from the same herd. However, tooth mineralisation in reindeer has never been explicitly investigated. Previous isotopic studies

of modern and archaeological reindeer have therefore estimated tooth mineralisation intervals based on other cervid species (Britton et al. 2009, 2011; Price et al. 2017; Piskorska et al. 2015; Gignoux et al. 2019), particularly the red deer (*Cervus elaphus*), fallow deer (*Dama dama*) and mule deer (*Odocoileus hemionus*) (Brown and Chapman 1991a, b; Rees et al. 1966), and it has been suggested that cervids as a group display similar periods of tooth development (Price et al. 2017). Notably, most of the previous work describing tooth mineralisation and eruption patterns has focused only on mandibular teeth while maxillary teeth remain relatively poorly characterised, obscuring any potential differences between the two. Here, we contrast our new Lubná reindeer data against enamel mineralisation models presented in Piskorska et al. 2015 (based on cervid comparisons and reindeer tooth eruption data), and Price et al. 2017 (based on intra-tooth isotopic analyses of Upper Palaeolithic reindeer). These two models are very similar, except that P4 is predicted to mineralise between 8 and 18 months by Piskorska et al. (2015), and between 13 and 18 months by Price et al. (2017).

### Stable isotope analysis

Stable isotope analyses of mammalian body tissues are a well-established means for investigating diet and migration patterns of past animals and humans, as well as the climatic context in which they lived. The methods are based upon the principle that body tissues record information about an individual's diet and environment relevant to the period in which the tissue formed (Wada et al. 1995: 7). Carbon ( $\delta^{13}\text{C}$ ) and nitrogen ( $\delta^{15}\text{N}$ ) stable isotope ratios in bone collagen reveal information about long term average dietary protein intake and trophic level (Ambrose 1993; Lee-Thorp 2008), and may also reveal information about the environmental

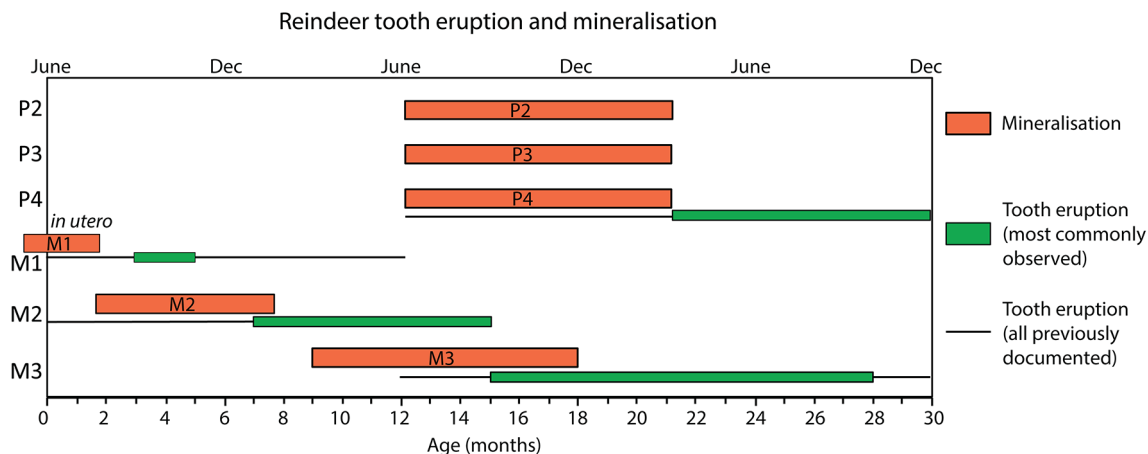


**Fig. 2** Reindeer tooth mineralisation and eruption intervals. Mineralisation intervals based on estimates from cervids, previous isotopic studies of reindeer and, for P2 and P3, the intra-tooth seasonality data

( $\delta^{18}\text{O}$  and  $\delta^{13}\text{C}$ ) reported in this study. Tooth eruption intervals are based on data from different reindeer populations (see main text for references)

context in which animals lived, such as whether they inhabited relatively open or closed environments, and whether conditions were wet, dry, hot, or cold (Farquhar et al. 1989; Craine et al. 2015). Similarly, stable carbon and oxygen ( $\delta^{13}\text{C}$  and  $\delta^{18}\text{O}$ ) isotope ratios from sequentially sampled tooth enamel carbonates can reveal seasonal differences in diet/environment and, away from the tropics, ambient seasonal air temperatures, and have been widely used to distinguish different seasons of growth within a single tooth (Sponheimer and Lee-Thorp 1999; Pederzani and Britton 2019).

Strontium isotope ratios ( $^{87}\text{Sr}/^{86}\text{Sr}$ ) in tooth enamel reflect the geological age and chemical composition of bedrock geology in the area where an individual lived during tissue formation.  $^{87}\text{Sr}$  is radiogenic and forms through radioactive decay of  $^{87}\text{Rb}$ , while  $^{86}\text{Sr}$  is stable and therefore its abundance is fixed. This causes the relative proportion of  $^{87}\text{Sr}$  to  $^{86}\text{Sr}$  in geological substrates to increase over time based on the age of the rock and its original rubidium content. Soluble strontium in rocks is released into the soil, vegetation and waters by weathering, and thus into the food chain where it becomes incorporated into skeletal tissues during growth. Enamel is resistant to post-mortem diagenetic changes and therefore preserves biogenic  $^{87}\text{Sr}/^{86}\text{Sr}$  data, but this is not the case for either bone or dentine, in which the original biogenic signature is overprinted in archaeological contexts with that of the local burial environment (Hoppe et al. 2003). Comparing strontium isotope ratios from enamel and dentine (or cementum) of a single tooth therefore provides a method for separating potential migrants from non-migrants within a sample population (Ericson 1985; Bentley 2006).

Previous analyses of reindeer bone collagen  $\delta^{13}\text{C}$  and  $\delta^{15}\text{N}$  have been widely reported, including from a number of European Middle and Upper Palaeolithic assemblages (Drucker et al. 2003, 2012; Stevens et al. 2008; Bocherens et al. 2011; Reade et al. 2020; Rivals et al. 2020; Britton et al. 2023). Intra-tooth  $^{87}\text{Sr}/^{86}\text{Sr}$  and  $\delta^{18}\text{O}$  data from modern and archaeological reindeer also exist from a number of previous studies. Seasonal variation in strontium, oxygen and carbon isotope ratios was observed in Late Pleistocene reindeer from Stellmoor and Meiendorf in northern Germany, corresponding to movements in an east-west direction across the North European Plain (Price et al. 2017). At the late Middle Palaeolithic site of Jonzac in southwest France, similarities in seasonal migration routes of three hunted reindeer were interpreted as individuals belonging to the same herd killed in close chronological succession in a small number of hunting episodes (Britton et al. 2011). And in the late Middle Palaeolithic site of Abri du Maras in southeast France, a plasticity in reindeer mobility patterns was observed, with three individuals appearing relatively sedentary and showing no evidence for seasonally-structured mobility, while a

single animal from another archaeological horizon showed clear evidence for summer-winter migratory behaviours over distances of at least 150–200 km (Britton et al. 2023). Meanwhile, results from the more recent site of Nunalleq in Alaska, dating to the Little Ice Age in the 15th to 17th centuries AD, showed seasonal migratory behaviour in all analysed individuals, but also suggested migrations ranged to various parts of the landscape over time (Gigleux et al. 2019). Another study of modern Alaskan caribou known to engage in high-fidelity seasonal herd movements year-on-year (based on radio-collared tracking data) confirmed that individuals from the same herd displayed the same general isotopic trends, even though some lived and died almost 10 years apart (Britton et al. 2009). Some inter-individual variability was nevertheless observed, reflecting individual behaviour, large herd sizes and the large geographic ranges involved.

### Dental Cementum analysis

Dental cementum is a bone-like tissue that grows from a single mineralisation point in incremental concentric layers around tooth roots. It holds the teeth in the periodontal ligament (Jones 1981) through mineralising collagen fibre bundles (Sharpey's fibres), which originate in the gum (Lieberman 1994: 525). It is deposited continuously from the point the tooth erupts and comes into occlusion, until either the death of the animal or the tooth falling out (Selvig 1963). Annual growth bands can be viewed in thin sections about 100  $\mu\text{m}$  thick (Lieberman 1994: 527). Acellular cementum is deposited relatively slowly and continuously toward the coronal end of the root and is well mineralised with an even structure (Davis 1986). It is a good indicator of both age and season of death (Morris 1972). Cellular cementum is found toward the apical end of the root and is deposited more rapidly, though it tends to be uneven and less mineralised (Garrett et al. 1981). Because of the uneven growth rate, it is good for estimating age-at-death but not season of death (Lieberman and Meadow 1992).

Acellular cementum bands under transmitted polarised light appear as thin parallel bands alternating between translucency and opacity (Lieberman 1994). Variation in the orientation of the collagen fibres (and thus the angle at which light is refracted) and the rate of mineralisation are the two main factors affecting the appearance of the bands (ibid.). Controlled studies showed that the orientation of the collagen fibres is affected by occlusal strain and mineralisation is affected by the nutritional content of the food. Therefore, assuming that an animal's quantity and quality of diet change seasonally, the translucent bands correspond to seasons of fast growth and opaque bands to seasons of slow growth, correlating with summer and winter

seasons (Lieberman 1994). Cementum in reindeer teeth is well-studied (Pike-Tay et al. 1999), and typically shows well differentiated seasonal banding reflecting the seasonal environments and pronounced dietary and nutritional shifts experienced by reindeer.

## Materials and methods

Nineteen teeth, mainly from the left maxilla from a minimum of seven individuals, plus two single M3s, were selected for strontium, oxygen and carbon isotope analysis (Table 1). None of the individuals retained a full set of teeth, and the specific elements sampled were chosen based on what was available. The minimum number of individuals (MNI) was initially calculated from dental element combinations and tooth wear patterns as seven; it was unclear at the time of sampling whether the loose M3s could also be different individuals, but as both teeth produced apparently unique isotopic profiles they are reported here separately, bringing the assumed MNI to nine. All sampled teeth were in wear. A subset of eleven teeth were further subjected to dental cementum analysis to establish the season of death. Additionally, ten fragments of cortical long bone were chosen at random from across the site for carbon and nitrogen

isotope analyses. The MNI of these samples is not known, but efforts were made to reduce the likelihood of sampling the same individual twice by deliberately targeting bone fragments from different grid squares across the excavated area.

To improve the bioavailable strontium isoscape basemap over the region of interest, five plant samples, two river water samples and one modern wild boar tooth were also analysed. Plant leaves (of mixed herbaceous species) were collected from fields and other locations with no recent agricultural activity in an attempt to negate any impact of fertilisers on the strontium signal. Water samples were collected directly from rivers, away from sewer pipes or other obvious sources of contamination. The analysed wild boar tooth was found in an area of woodland and is presumed to derive from natural death.

## Strontium isotope analysis of teeth

Strontium isotope analysis was undertaken following the procedures detailed in Pryor et al. 2020a and summarised here. For each tooth, an enamel-dentine strip approximately 3 mm wide running from the crown tip to the root was removed by hand using a diamond-encrusted circular saw. The resulting strips ranged in length from 6 to 16 mm, depending on tooth wear. Strontium isotope ratios were measured along the mid-line of the enamel cross-section from occlusal surface to root using laser ablation multi-collector inductively coupled plasma mass spectrometry (LA-MC-ICP-MS). LA-MC-ICP-MS can be used to measure enamel  $^{87}\text{Sr}/^{86}\text{Sr}$  ratios at high spatial resolution and has seen increasing use in recent years (e.g. Gerling and Lewis 2017; Lugli et al. 2017, 2019; Pryor et al. 2020a, b; Lazzarini et al. 2021). The technique has the potential to reveal evidence of mobility at fine temporal resolutions, recently demonstrated in the context of modern goats with known mobility patterns, which confirmed the visibility of movements on timescales of about 45 days (Lazzarini et al. 2021). A small strip of dentine was also analysed from a subset of the Lubná teeth in order to obtain a measure of the local bioavailable strontium isotope signature at the burial site.

Strontium isotope ratios were measured using a Thermo Scientific Neptune MC-ICP mass spectrometer coupled to a New Wave 193 nm Ar-F excimer laser ablation system (UP193FX) at the National Oceanography Centre, University of Southampton. Prior to data collection, the enamel and dentine targeted for analysis was pre-ablated to remove surface contaminants. The laser settings used for data collection were as follows: a laser beam diameter of 150  $\mu\text{m}$ , repetition rate of 15 Hz, and tracking speed of 15  $\mu\text{m}\text{s}^{-1}$ . The ablated sample was swept from the laser cell using

**Table 1** Teeth sampled for strontium, oxygen and carbon isotope analysis and dental cementum analysis

Individual	Sample ID	Element	Grid square	Find number	Dental cementum analysis
1	LB2	RM <sub>3</sub>	E5/C	216	
	LB3	RM <sub>2</sub>			X
2	LB5	LP <sup>3</sup>	E6/A	1264	X
	LB6	LP <sup>4</sup>			
	LB7	LM <sup>1</sup>			
	LB8	LP <sup>2</sup>			X
3	LB9	LP <sup>3</sup>	E7/D	1021	
	LB10	LP <sup>4</sup>			X
	LB11*	LM <sup>1</sup>			X
	LB12	LM <sup>3</sup>			X
	LB13	LM <sup>2</sup>			
4	LB14	LP <sup>4</sup>	E7/D	1008	
	LB15	LP <sup>3</sup>			X
5	LB16	LP <sup>3</sup>	E6/B	1168	
	LB17	LP <sup>4</sup>			X
6	LB18	LP <sup>4</sup>	E6/C	1320	X
	LB19	LP <sup>3</sup>			X
7	LB20	LM <sup>3</sup>	E6/C	1320	
	LB21	LM <sup>1</sup>			
	LB22	LM <sup>2</sup>			
8	LB1	RM <sub>3</sub>	E7/C	685	X
9	LB4	RM <sub>3</sub>	G7/A	1738	

\* LB11 was later withdrawn from isotopic analyses due to high levels of tooth wear.

helium gas, which was then mixed with argon and nitrogen gas flows before entering the plasma ion source. The  $^{87}\text{Sr}/^{86}\text{Sr}$  ratio was measured in static collection mode with an integration time of 1.049 s using a tuned mass spectrometer setup designed to reduce oxide production (de Jong et al. 2007; de Jong 2013; Lewis et al. 2014: 175). Oxide formation (monitored as  $^{254}(\text{UO})+^{238}\text{U}+$ ) was minimised through careful control of plasma conditions (de Jong 2013; Lewis et al. 2014; Willmes et al. 2016). An on-peak gas blank correction for  $^{86}\text{Kr}$  interference was applied to all masses, then ratios were corrected for mass fractionation using an  $^{86}\text{Sr}/^{88}\text{Sr}$  ratio of 0.1194 according to an exponential mass fractionation law (Russell et al. 1978).  $^{89}\text{Y}$  was monitored as a proxy for rare earth element contamination and any data showing significant concentrations were disregarded (de Jong 2013; Woodhead et al. 2005), aside from a small number of instances where evidence indicated that the biogenic  $^{87}\text{Sr}/^{86}\text{Sr}$  ratio was retained. Isobaric interference from  $^{87}\text{Rb}$  was corrected for using the natural  $^{87}\text{Rb}/^{85}\text{Rb}$  ratio of 0.386481 (Faure 1986).

Repeat analyses bracketing the archaeological samples of an in-house enamel standard prepared from a pig fed exclusively marine foods and measured by Thermal Ionisation Mass Spectrometry (TIMS) to 0.709078 showed an offset of  $+79 \pm 81$  parts per million ( $1\sigma$ ) for the laser ablation analyses over the TIMS values. This is well within the precision of individual measurements of  $\sim 200$ – $600$  ppm and the total variation within the teeth of  $>4260$  ppm, and is therefore considered insignificant to our interpretation of the data. The  $^{84}\text{Sr}/^{86}\text{Sr}$  ratio in all measured samples fell very close to the expected value of 0.0565 (Thirlwall 1991; Supplementary Tables 3 and 4). Any data that showed significant deviations were discarded.

### Strontium analysis of plant and water basemap samples

Five plant and two water samples were analysed by TIMS at the National Oceanography Centre, University of Southampton. Plant samples were prepared by rinsing with ultrapure water to remove surface contamination. All plant and water samples were then freeze dried and dissolved at  $130^\circ\text{C}$  overnight in concentrated sub boiled (SB)  $\text{HNO}_3$ , followed by the addition of 2 ml of  $\text{H}_2\text{O}_2$  and heating at  $80^\circ\text{C}$  overnight. Pure strontium was isolated from the samples using an  $\sim 50$   $\mu\text{L}$  ion exchange chromatography column of Sr-Resin<sup>®</sup> resin (Triskem International, Bruz, France), and co-loaded onto a tantalum filament with 1  $\mu\text{L}$  of an activator solution containing  $\text{TaO}$ ,  $\text{H}_3\text{PO}_4$  and trace HF. The loaded filaments were analysed with a ThermoFisher Triton Plus Thermal Ionisation Mass Spectrometer using a 5-collector static procedure. The results were corrected for fractionation

using an exponential normalisation with  $^{86}\text{Sr}/^{88}\text{Sr}$  of 0.1194. The long-term precision and accuracy was determined by repeated measurements of an international standard (NIST SRM987) with an average value of  $0.710247 \pm 0.000024$  on 117 repeats over a 3.5 year period including these analyses.

### Enamel carbonate oxygen and carbon

Enamel carbonate samples were collected from locations immediately adjacent to the strontium isotope sample region. In one case, LB16, tooth morphology made this strategy impossible so carbonate samples were collected from the opposite side of the tooth instead. For each tooth, the enamel surface was abraded prior to sampling using a diamond-tipped burr to expose a clean enamel surface. Sequential samples of 3–5 mg of enamel powder were then drilled at 2–3 mm intervals along the growth axis of the tooth cusp using a 1 mm diamond-tipped drill bit. This method generated a total of 95 samples for analysis, of which 11 were analysed twice to check consistency of measurement; duplicates were then averaged to produce a final value used for interpretation. Enamel powders were pre-treated by soaking in 0.1 M acetic acid at room temperature for ten minutes to remove any exogenous carbonates (Pellegrini and Snoek 2016). Between 0.5 and 0.6 mg of powder was then reacted with 106% phosphoric acid at  $90^\circ\text{C}$  using a Kiel IV carbonate preparation system at the National Oceanography Centre, University of Southampton. The resulting  $\text{CO}_2$  was analysed using a Thermo Scientific MAT253 dual inlet isotope ratio mass spectrometer. Isotope ratio data are reported as  $\delta$  values in ‰ with reference to the VPDB isotopic standard for  $\delta^{18}\text{O}$  and  $\delta^{13}\text{C}$ . Replicates of IAEA (International Atomic Energy Agency) standards NBS18 and NBS19, and an in-house laboratory standard made from Upper Palaeolithic mammoth tooth enamel show that the precision is better than  $\pm 0.2\text{‰}$  for  $\delta^{18}\text{O}$  and better than  $0.1\text{‰}$  for  $\delta^{13}\text{C}$ . The mean standard deviation for the 11 Lubná enamel samples analysed twice was  $<0.2\text{‰}$  for both  $\delta^{18}\text{O}$  and  $\delta^{13}\text{C}$ .

### Bone collagen carbon and nitrogen

Bone chunks weighing between 0.5 and 1 g were cut from the sampled bones and cleaned with silicon carbide abrasive. Collagen was extracted using a modified Longin (1971) method. Bones were demineralised in 0.5 M hydrochloric acid (HCl) for 2–3 weeks, replacing the acid every few days. Samples were then rinsed in de-ionised water and gelatinised in pH 3 water at  $75^\circ\text{C}$  for 48 h. The supernatant liquid was filtered using an Ezee filter with 60–90  $\mu\text{m}$  pore size (Elaky Laboratories Ltd), frozen and freeze dried.  $0.8 \pm 0.1$  mg of collagen was then weighed into tin capsules and analysed in duplicate using a Sercon Integra2 isotope

ratio mass spectrometer at the Environment and Sustainability Institute, University of Exeter. The results are reported as means and standard deviations calculated from the duplicate analyses using standard delta ( $\delta$ ) notation in parts per thousand (‰) relative to the standards Vienna Pee Dee Belemnite (VPDB) for  $\delta^{13}\text{C}$  and Ambient Inhalable Reservoir (AIR) for  $\delta^{15}\text{N}$  respectively. Analytical uncertainty was calculated as  $<0.08$  for  $\delta^{13}\text{C}$  and  $<0.18$  for  $\delta^{15}\text{N}$  ( $2\sigma$ ) based on repeat analysis of internal standards bracketing the sample analyses and defined previously with respect to IAEA-N-1, IAEA-N-2, IAEA-LSVEC, IAEA-CH-6 and B2155 international standards; repeat analyses of the archaeological samples showed maximum differences of  $<0.2\%$  between replicates.

### Dental Cementum

Fifteen horizontal sections were cut from 11 teeth of 7 individuals (Table 1). The sections were embedded in Epofix<sup>©</sup> epoxy resin, ground with 90  $\mu\text{m}$  and 30  $\mu\text{m}$  grit paper to create a fresh cross-section and mounted on glass slides with Loctite 358 adhesive. The thin sections were cut using a Kemet Geoform thin section machine to a thickness of approximately 110  $\mu\text{m}$  and then polished by hand on a 30  $\mu\text{m}$  grit paper and 1  $\mu\text{m}$  aluminum oxide powder until the microstructures were clearly visible under a microscope. Sections were analysed with the aid of a  $\lambda$  filter under transmitted plain and cross-polarised light at x25, x50, x100, x200 and x500 magnification.

## Results

### Collagen $\delta^{13}\text{C}$ and $\delta^{15}\text{N}$

Atomic C: N ratios for all samples fell between 3.23 and 3.34, well within the accepted range for well-preserved collagen of 2.90–3.60 (DeNiro 1985). Good collagen preservation is also indicated by %C yields of 29.3% or higher and

%N yields of 10.2% or higher (Table 2; Ambrose 1990). The Lubná reindeer collagen data are tightly clustered with means and standard deviations of  $-19.1 \pm 0.3$  in  $\delta^{13}\text{C}$  and  $2.5 \pm 0.5$  in  $\delta^{15}\text{N}$ . These results are similar to those measured on reindeer from other Upper Palaeolithic sites in Czechia (Bocherens et al. 2015; Reade et al. 2021) and the European mammoth steppe region more generally (Bocherens 2015; Schwartz-Narbonne et al. 2019). Reindeer collagen  $\delta^{13}\text{C}$  is typically slightly higher than that of other contemporary herbivore species, a pattern widely attributed to seasonal lichen consumption (e.g. Drucker et al. 2015; Bocherens et al. 2015), and this is likely to also be the case at Lubná. Meanwhile, the  $\delta^{15}\text{N}$  values fall at the lower end of the range typically observed in European Upper Palaeolithic reindeer (Schwartz-Narbonne et al. 2019), probably reflecting cold, damp soils and extensive permafrost cover around Lubná — and Central Europe more generally — at the time the reindeer lived (Lindgren et al. 2016; Drucker et al. 2011; Rabanus-Wallace et al. 2017).

### Geology and strontium basemap

Bohemia is a geologically complex region that mixes old and young marine-derived and terrestrial rock formations, including some recent volcanic bodies and Quaternary loess deposits, each of which may show distinctive strontium isotope ratios, with potential for high isotopic variability within and between sampled reindeer (Bentley et al. 2012; Price et al. 2004). Accordingly, new data from five modern plant samples, two water samples and a modern wild boar tooth (Table 3), together with existing data, indicate distinct regional patterning useful for revealing the mobility patterns of the Lubná reindeer (Fig. 3; Supplementary Table 2; Supplementary Fig. 4).

Lubná VI lies within Pleistocene loess, deposits of which are present in patches throughout the study region. Existing data from human and animal bones from loessic sites in the Bohemian-Moravian foothills indicate a bioavailable strontium isotope range of between 0.7093 and 0.7108 for

**Table 2** Summary of Lubná reindeer bone collagen data. Each sample was analysed in duplicate (raw data are provided in supplementary Table 1)

Sample	Excavation square	Find number	Collagen yield (%)	$\delta^{15}\text{N}$		$\delta^{13}\text{C}$	
				mean	s.d	mean	s.d
Lub 18_1	D5/D	1450	11.9	2.8	0.1	-19.2	0.1
Lub 18_2	F7/B	503	10.4	2.9	0.0	-19.5	0.1
Lub 18_3	E7/C	1195	9.6	1.8	0.0	-18.7	0.1
Lub 18_4	B5/B	1358	8.2	2.5	0.0	-18.8	0.1
Lub 18_5	F7/A	506	8.8	1.9	0.1	-19.0	0.1
Lub 18_6	F6/B	357	7.8	2.7	0.0	-19.3	0.1
Lub 18_7	F8/C	316	4.7	2.3	0.1	-18.7	0.1
Lub 18_8	E5/C	223	9.0	3.0	0.0	-19.2	0.0
Lub 18_9	F7/A	509	6.3	2.8	0.0	-18.6	0.1
Lub 18_10	G5/C	1517	9.9	1.8	0.1	-19.5	0.1



**Table 3** New data describing bioavailable  $^{87}\text{Sr}/^{86}\text{Sr}$  variability across Bohemia. Sample LubP10 was measured by LA-MC-ICPMS. Plant and water samples were measured by TIMS

Map code	Sampe ID	Longitude	Latitude	Location	Material	$^{87}\text{Sr}/^{86}\text{Sr}$	$\pm 2$ SE
10	LubP1	14.23	50.88	Hřensko	Plant	0.711091	0.000034
15	LubP3	16.37	50.33	Deštné v Orlických horách	Plant	0.709742	0.000012
16	LubP4	16.09	50.21	Bolehošť	Plant	0.709366	0.000012
12	LubP5	14.01	50.58	Radejčín	Plant	0.704873	0.000012
10	LubP8	14.23	50.88	Elbe (Czech/German border)	River water	0.711332	0.000014
18	LubP9	16.06	50.14	Orlice (Týniště nad Orlicí)	River water	0.709896	0.000018
19	LubP10	16.07	50.11	Žďár nad Orlicí	Tooth enamel	0.708208	0.000148
20	SR39	15.82	49.10	Dolní Lažany	Plant	0.713515	0.000015

these deposits (Price et al. 2004; Scheeres et al. 2014). To the north, in the low-lying Bohemian Cretaceous basin, new and existing data from plants and river waters indicate a slightly less radiogenic bioavailable  $^{87}\text{Sr}/^{86}\text{Sr}$  range of 0.70846–0.70989. A modern wild boar tooth (LubP10) from a woodland near the Orlice river on the eastern margins of the basin produced a mean value of  $0.70821 \pm 0.00015$ , slightly lower than the range observed in the plants and river waters. These weakly radiogenic values are as expected from marine-derived Cretaceous sediments with predicted initial  $^{87}\text{Sr}/^{86}\text{Sr}$  values between 0.7073 and 0.7078 (McArthur et al. 2012). Meanwhile, loess in the Czech/German border area falls within a similar but slightly elevated range of 0.711091–0.711332, attested by one new plant sample and one new river water sample from the Elbe Sandstone Mountains (LubP1, LubP8). Further north and west, in SE Germany (Saxony), the loess deposits become more radiogenic, consistently producing high initial (bulk) readings and bioavailable values of around 0.7117–0.7144 (Voerkelius et al. 2010; Rousseau et al. 2014; Gerling 2015).

Looking northwest of Lubná, the Ohře river valley and associated Neogene basalt uplands of the České Středohoří (Central Bohemian Highlands) are characterised by the most weakly radiogenic sediments in the region with bioavailable  $^{87}\text{Sr}/^{86}\text{Sr}$  of around 0.704–0.7093. Bulk whole-rock data from outcroppings of other Neogene basalts scattered across the wider Bohemian region are also shown in Fig. 3 for completeness, demonstrating low initial values of between 0.70312 and 0.70355 (Bendl et al. 1993), although these appear to have had minimal impact on bioavailable values measured locally to the outcroppings in mineral waters, plants, and archaeological humans and fauna located close by.

The highland regions south of Lubná, including the Carlsbad Highlands, Brdy and the Bohemian-Moravian highlands, are dominated by older Precambrian and Carboniferous granites, gneisses, slates, shales and sandstones which all typically demonstrate strongly radiogenic values above 0.712 wherever data are available (Fiala et al. 2014; Bentley and Knipper 2005; Voerkelius et al. 2010; Möller et al. 1998). Although data are scarce across much of the

Bohemian-Moravian highlands, a single new plant sample (Sr39) from the SE part of the highlands confirms the radiogenic nature of these deposits with an  $^{87}\text{Sr}/^{86}\text{Sr}$  ratio of 0.713515.

### Dentine $^{87}\text{Sr}/^{86}\text{Sr}$

Dentine  $^{87}\text{Sr}/^{86}\text{Sr}$  ratios from 10 teeth from six reindeer fell within a range of 0.71026–0.71108 (calculated as a median of  $0.71067 \pm 1.5\%$  the IQR of 0.00027; Supplementary Table 3). Data from three further teeth were excluded from these calculations due to (i) inaccurate  $^{84}\text{Sr}/^{86}\text{Sr}$  ratios suggesting unreliable results (LB1); (ii) high yttrium content (LB6); or (iii) because the  $^{87}\text{Sr}/^{86}\text{Sr}$  ratios varied substantially along the length of the measured dentine profile, indicating that the dentine had not fully equilibrated with the local surrounding geology (LB19) (Supplementary Information file 2). These dentine results fall well within the range identified for Pleistocene loess in the central Bohemian Massif east of Lubná (Fig. 3), confirming the isotopic similarity of loess deposits more generally throughout this region.

### Enamel $^{87}\text{Sr}/^{86}\text{Sr}$

The enamel strontium dataset is complex and reveals detailed information about the behaviour of the Lubná reindeer (Fig. 4). Enamel  $^{87}\text{Sr}/^{86}\text{Sr}$  ranged from 0.70873 to 0.71177, although only three individuals produced values substantially below 0.710 (reindeer 4, 6 and 7). The  $^{87}\text{Sr}/^{86}\text{Sr}$  profiles for reindeer 4, 6, and 9 show minimal variability and are essentially static, consistent with mobility within a single geological region during the time captured by the enamel profiles. Only two reindeer produced data consistent with living in the local Lubná range for all, or nearly all, of the period of tooth growth (individuals 5 and 9). Meanwhile, six reindeer (individuals 1, 2, 3, 5, 7 and 8) recorded often abrupt variations in the  $^{87}\text{Sr}/^{86}\text{Sr}$  profiles indicating movements across isotopically distinct geologies (Fig. 4). These movement events can mostly be directly observed in the enamel data although, for individual 7, at least one mobility event occurred between the end of M2 growth and

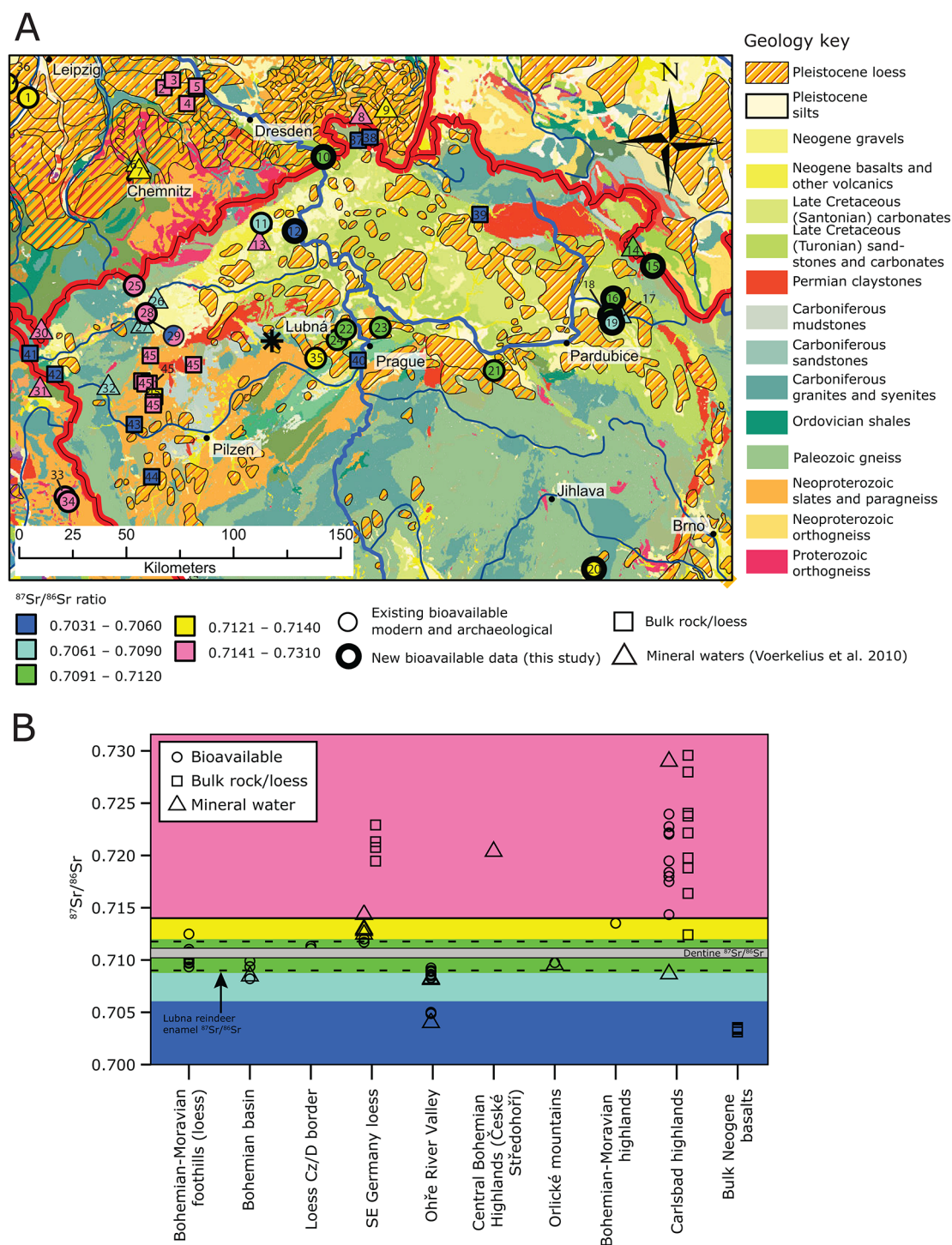
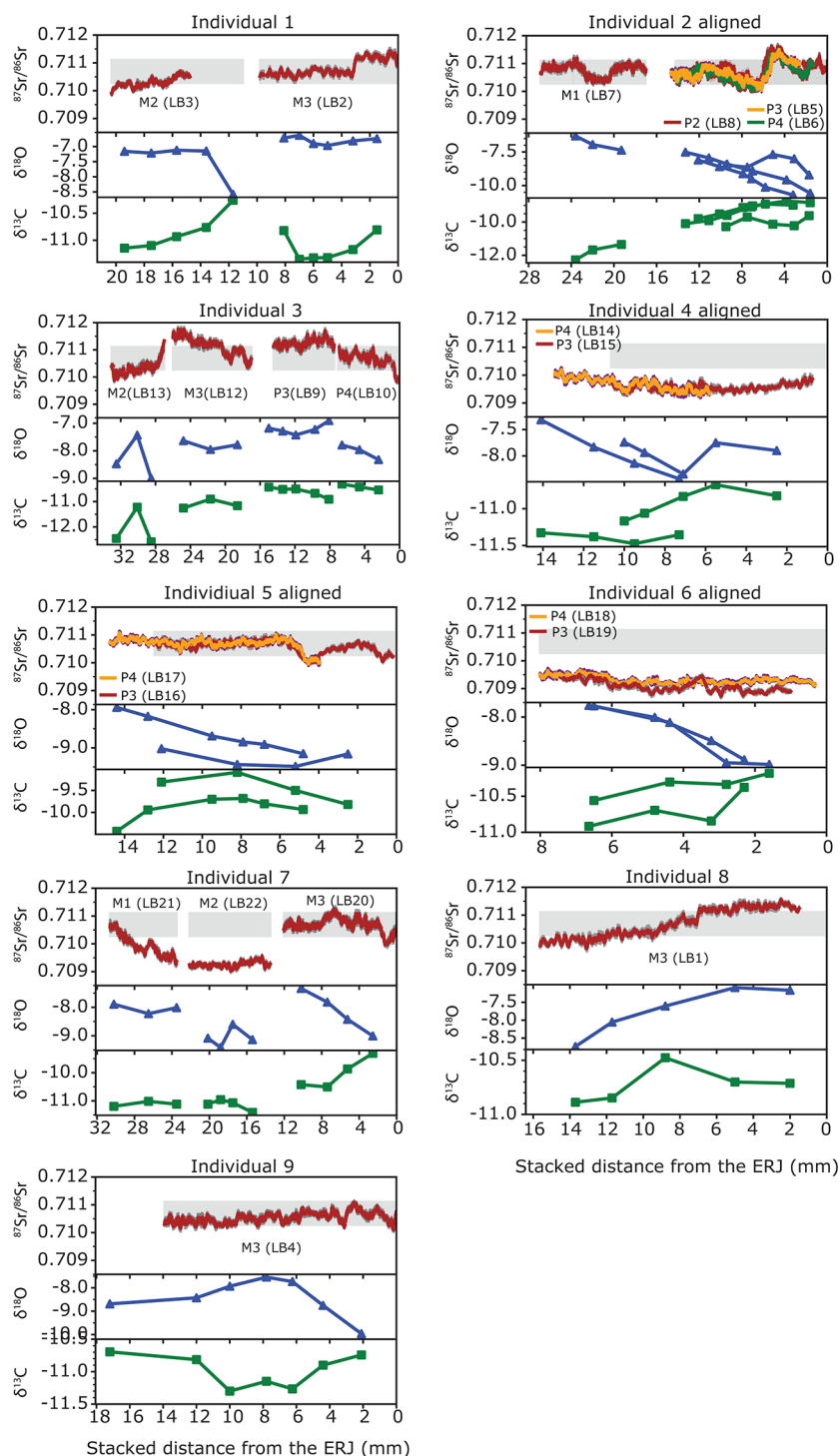


**Fig. 3** Geology and strontium isotope variation in Bohemia. **(a)** Geological map and location of datapoints describing strontium isotope variation in the region, colour-coded according to the  $^{87}\text{Sr}/^{86}\text{Sr}$  ratio. Details for each numbered site can be found in Supplementary Table 2. **(b)** Summary of strontium isotope ratio base-mapping data by region, colour-coded using the same  $^{87}\text{Sr}/^{86}\text{Sr}$  ranges as panel (a). The grey-

shaded bar indicates the  $^{87}\text{Sr}/^{86}\text{Sr}$  range of Lubná reindeer dentine, and the dotted lines indicate the maximum range recorded in the Lubná reindeer enamel, falling entirely within the green-shaded  $^{87}\text{Sr}/^{86}\text{Sr}$  range. See Supplementary Tables 2 and Supplementary Figure S4 for further details of basemapping sites by geographic region

**Fig. 4** Enamel strontium, oxygen and carbon isotope ratio data from the Lubná reindeer.  $^{87}\text{Sr}/^{86}\text{Sr}$  profiles are shown as a 10-point mean running average of the individual laser ablation measurements. Dark grey shading around the lines indicates the uncertainty of measurement defined as the standard error (1SE), although this is mostly hidden by the thickness of the  $^{87}\text{Sr}/^{86}\text{Sr}$  profile line. The light grey bar indicates the local bioavailable strontium range for Lubná as defined by the tooth dentine. Consecutively-forming teeth from the same individual are shown using a cumulative “distance from the enamel-root junction” (stacked x-axis), with the addition of a small gap of arbitrary length inserted between different elements to make clear where each tooth profile starts and finishes. Simultaneously-forming teeth (P2, P3 and P4 elements) were aligned visually by wiggle matching to obtain a close fit across the datasets, and are also shown using a stacked x-axis. Further dataplots showing the  $^{88}\text{Sr}$ ,  $^{84}\text{Sr}/^{86}\text{Sr}$  and  $^{85}\text{Rb}/^{86}\text{Sr}$  data from each sampled tooth are shown in Supplementary Information file 3



the start of the M3 profile that was not directly captured by the enamel available for analysis (most likely due to wear of the M3). Abnormal spikes of  $^{89}\text{Y}$  were observed in teeth LB8 and LB19 (Supplementary Information file 3), but in the absence of any discernible impact in the  $^{87}\text{Sr}/^{86}\text{Sr}$  profiles these sections were retained as part of our analysis. Plots of the cleaned raw data for each molar element are given in Supplementary Information file 3.

### Enamel $\delta^{18}\text{O}$ and $\delta^{13}\text{C}$

Enamel  $\delta^{18}\text{O}$  varied between a total range of  $-10.7\%$  and  $-6.3\%$ , while the intra-tooth range varied between  $0.3\%$ – $3.0\%$  (Table 4; Supplementary Table 5). Enamel  $\delta^{13}\text{C}$  varied between a total range of  $-12.6\%$  and  $-8.7\%$ , while the intra-tooth range varied between  $0.2\%$ – $1.4\%$  (Table 4; Supplementary Table 5). This scale of intra-tooth variability is

**Table 4** Summary of intra-tooth enamel  $\delta^{18}\text{O}$  and  $\delta^{13}\text{C}$  data

Individual	Tooth	N of samples	$\delta^{13}\text{C}$			$\delta^{18}\text{O}$		
			Min	Max	Range	Min	Max	Range
1	LB2	5	-11.2	-10.3	0.9	-8.6	-7.1	1.5
	LB3	6	-11.4	-10.8	0.5	-7.0	-6.6	0.3
2	LB5	6	-9.8	-8.9	0.9	-10.7	-8.1	2.6
	LB6	6	-10.1	-8.7	1.4	-10.6	-7.5	3.1
	LB7	3	-12.3	-11.4	0.9	-7.4	-6.3	1.1
	LB8	5	-10.3	-9.6	0.7	-9.2	-7.7	1.5
3	LB9	5	-10.9	-10.4	0.5	-7.4	-6.9	0.5
	LB10	3	-10.5	-10.3	0.2	-8.3	-7.8	0.5
	LB12	3	-11.3	-10.9	0.4	-8.0	-7.6	0.3
	LB13	3	-12.6	-11.2	1.4	-9.0	-7.4	1.6
4	LB14	4	-11.5	-11.3	0.2	-8.4	-7.3	1.1
	LB15	5	-11.2	-10.7	0.5	-8.3	-7.7	0.6
5	LB16	4	-9.8	-9.1	0.7	-9.5	-9.0	0.5
	LB17	6	-10.4	-9.7	0.8	-9.2	-7.9	1.2
6	LB18	4	-10.6	-10.2	0.4	-9.0	-7.8	1.2
	LB19	4	-10.9	-10.4	0.5	-8.9	-7.8	1.1
7	LB20	4	-10.5	-9.3	1.2	-9.0	-7.3	1.7
	LB21	3	-11.2	-11.0	0.2	-8.2	-7.9	0.3
	LB22	4	-11.4	-11.0	0.4	-9.4	-8.6	0.8
8	LB1	5	-10.9	-10.5	0.4	-8.7	-7.1	1.7
9	LB4	7	-11.3	-10.7	0.6	-10.0	-7.5	2.4

directly comparable to that observed previously in modern and archaeological reindeer teeth, including from European Upper Palaeolithic contexts (Britton et al. 2009; Gignoux et al. 2019; Price et al. 2017). The data from individual teeth mostly form smooth lines or curves, as expected for intra-tooth data. A weaning effect is clearly visible in the M1 of Reindeer 2 (LB7), where  $\delta^{18}\text{O}$  is higher and  $\delta^{13}\text{C}$  is lower relative to the other measured teeth in this individual, reflecting consumption of fat-rich maternal milk during the M1 formation interval (Wright and Schwarcz 1998; Price et al. 2017 and references therein). Isotopic variability in the remaining teeth most likely reflects seasonal climatic changes experienced by the Lubná reindeer. An exception is LB13, a root-etched M2 from individual 3, where neither the  $\delta^{18}\text{O}$  nor  $\delta^{13}\text{C}$  profiles show the expected trends and the  $\delta^{13}\text{C}$  lies outside the range seen in other teeth from this individual (Figs. 4 and 5). Given the root etching affecting this tooth, carbonate data from LB13 were considered as diagenetic and disregarded when making interpretations.

Reindeer 2 and 5 have markedly lower  $\delta^{18}\text{O}$  and higher  $\delta^{13}\text{C}$  values in their P3–P4s compared to all other teeth (Fig. 5). The pattern is particularly apparent in the  $\delta^{13}\text{C}$  profiles, and is also observed to a lesser extent in Reindeer 7 ( $\delta^{13}\text{C}$ ) and the single M3 of Reindeer 9 ( $\delta^{18}\text{O}$ ), which produced the largest  $\delta^{18}\text{O}$  span of any tooth in the whole dataset. All four of these reindeer have  $^{87}\text{Sr}/^{86}\text{Sr}$  profiles associated with year-round residency in the vicinity of Lubná or the Bohemian-Moravian foothills region more generally (see later), together indicating that at least some parts of this

region experienced a more extreme winter climate and that reindeer living in these conditions consumed a specific winter diet heavily enriched in lichen (Drucker et al. 2001).

### Quantitative temperature reconstruction

In a European Pleistocene context, enamel  $\delta^{18}\text{O}$  is directly related to air temperatures during the period of tooth formation. Intra-tooth data can therefore potentially be calibrated to obtain quantitative estimates of temperature changes experienced by individual animals. However, the required calibrations are not straight forward; tooth enamel formation is a complex two-phase process that attenuates seasonal variations in  $\delta^{18}\text{O}$ , which must be accounted for (e.g. Zazzo et al. 2012). Recent studies have approached this problem using sophisticated mathematical models tuned to specific species to estimate the original seasonally-resolved signals registered in the teeth (e.g. Passey et al. 2005; Green et al. 2018; Uno et al. 2020; Pederzani et al. 2021a, b). Unfortunately, these models require detailed knowledge of tooth mineralisation parameters that are not yet established for reindeer, so cannot be applied here. A more straightforward and simplified calculation of estimated mean annual temperature was therefore attempted by converting an average of  $\delta^{18}\text{O}_{\text{PDB}} = -8.5\text{‰}$  to the equivalent value on the SMOW reference scale, and then making a series of calibrations from  $\delta^{18}\text{O}_{\text{carbonate}}$  to  $\delta^{18}\text{O}_{\text{phosphate}}$  to  $\delta^{18}\text{O}_{\text{precipitation}}$  (using equations from Coplen et al. 1983; Iacumin et al. 1996; Longinelli et al. 2003). However, these calculations estimated

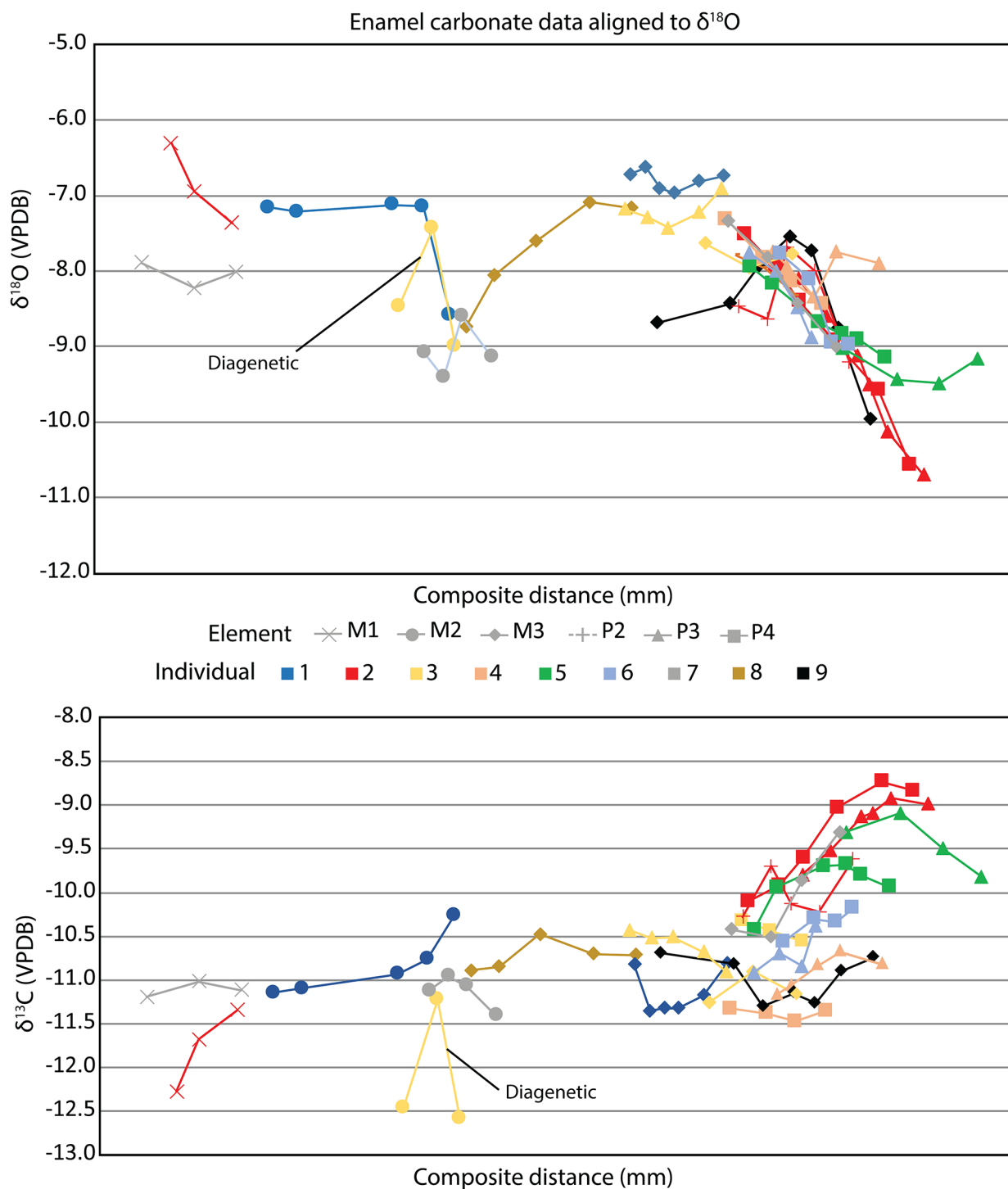


**Fig. 5** Intra-tooth  $\delta^{18}\text{O}$  and  $\delta^{13}\text{C}$  stable isotope data plotted using a composite (stacked) x-axis. The data from each tooth were first sorted by order of tooth mineralisation (Fig. 2b) and then aligned visually

without any adjustment or scaling to obtain a good fit (giving preference to alignments in  $\delta^{18}\text{O}$ )

$\delta^{18}\text{O}_{\text{precipitation}}$  to be marginally more positive (i.e. indicating warmer climates) than that in Central Europe today, wholly unrealistic for climates of Upper Palaeolithic Europe approaching the Last Glacial Maximum. We also tested a recalculated  $\delta^{18}\text{O}_{\text{phosphate}} - \delta^{18}\text{O}_{\text{precipitation}}$  relationship based

on Longinelli et al.'s data that excluded all bone phosphate data and used only data from enamel phosphates (Stevens and Reade 2021), however the resulting  $\delta^{18}\text{O}_{\text{precipitation}}$  estimates for Lubná remained indistinguishable from modern

precipitation and therefore indicating an implausibly mild climate.

It is not currently clear why the isotopic calibrations indicated  $\delta^{18}\text{O}_{\text{precipitation}}$  estimates this high. The  $\delta^{18}\text{O}_{\text{PDB}} - \delta^{18}\text{O}_{\text{SMOW}}$  conversion represents a change of units and the associated errors are negligible (Pryor et al. 2014). However, it is possible that the  $\delta^{18}\text{O}_{\text{carbonate}} - \delta^{18}\text{O}_{\text{phosphate}} - \delta^{18}\text{O}_{\text{precipitation}}$  calibrations in reindeer are not yet sufficiently well defined. Multiple studies have demonstrated that the  $\delta^{18}\text{O}_{\text{carbonate}} - \delta^{18}\text{O}_{\text{phosphate}}$  relationship is complex, with suggestions that a species-specific relationship is required for conversions to be done appropriately (none yet exists for reindeer), or that the two proxies may not be completely equivalent due to different attenuation and averaging effects in  $\delta^{18}\text{O}_{\text{carbonate}}$  and  $\delta^{18}\text{O}_{\text{phosphate}}$  phases of the same sample (Pellegrini et al. 2011; Martin et al. 2008). Meanwhile, the reindeer-specific  $\delta^{18}\text{O}_{\text{phosphate}}$  to  $\delta^{18}\text{O}_{\text{precipitation}}$  calibration was based on populations with very high intra-population variability (see discussion in Longinelli et al. 2003), and it is possible this variability has affected the accuracy of the calculated quantitative relationship. We therefore caution against using the Lubná reindeer data to make quantitative temperature estimates until the required calibration equations have been improved and verified. We also note that previous studies reporting Upper Palaeolithic reindeer  $\delta^{18}\text{O}_{\text{carbonate}}$  data have avoided such temperature estimations as well (e.g. Price et al. 2017).

### Seasonality of tooth formation

Intra-individual isotopic profiles mostly align well between molar elements and show good overall agreement with the tooth mineralisation/eruption models presented by Piskorska et al. (2015) and Price et al. (2017). Accordingly, Lubná reindeer M1 and M2 teeth formed sequentially during the summer, autumn and early winter seasons of the first year of life, consistent with a late spring or early summer birthing period. M3 teeth formed between approximately 9–18 months of age, beginning around the time that M2 growth ended, coinciding with spring-summer-autumn. Instances where the  $\delta^{18}\text{O}$  and  $\delta^{13}\text{C}$  data do not align between M2–M3 are most likely due to wear of the M3 erasing the earliest-forming part of the profile in this tooth (e.g. individual 1).

P3–P4 combinations are available for five individuals. In four of these (reindeer 2, 4, 5 and 6) the strontium, oxygen and carbon isotope profiles align closely between the two premolars, particularly the fluctuations in  $^{87}\text{Sr}/^{86}\text{Sr}$  profiles (Fig. 4). Some variability in the absolute values of  $\delta^{18}\text{O}$  and  $\delta^{13}\text{C}$  are apparent, but the shape of the curves still clearly identifies the seasonal changes in each element and indicate that P3 and P4 both formed in the summer-autumn-winter of the second year of life, with mineralisation finishing a

few months after M3. Where differences in absolute values of  $\delta^{18}\text{O}$  and  $\delta^{13}\text{C}$  occur, these are most likely due to specific tooth geometry at the sampling location, and isotopic averaging effects introduced during the two-phase enamel mineralisation process. Unexpectedly, our data also suggest that the order in which P3 and P4 mineralise may not be consistent in every case. In reindeer 4 and 5, P3 appears to finish mineralising later than P4. However, the opposite is true for reindeer 2 and 6 where P4 apparently finished mineralising marginally later. Further, in reindeer 3, the isotopic profiles for P3–P4 show no obvious overlap at all; this indicates either that P3 and P4 formed sequentially in this individual with no overlap in mineralisation intervals, or that these teeth, which were excavated close to each other but as separate elements, in fact belong to two different individuals. Given this uncertainty we do not make any specific interpretations of the P3–P4 data from reindeer 3. However, we note the inconsistent timing of P3–P4 formation more generally as a point for investigation in future studies.

The strontium isotope profile from the only analysed P2 (from reindeer 2) matches closely with the P3–P4 from the same individual. This is consistent with a P2 formation time in the second year of life as observed in other cervids (Brown and Chapman 1991a, b). A deviation in the  $\delta^{13}\text{C}$  and  $\delta^{18}\text{O}$  profiles of this P2 is visible with respect to the P3–P4 data (Fig. 4), most likely caused by tooth geometry and averaging effects during mineralisation at the sampling location.

In summary, in comparison to previous models of reindeer tooth mineralisation presented in Piskorska et al. (2015) and Price et al. (2017), our data agree with Piskorska regarding six-to-nine month mineralisation times for P3 and P4, and suggest more variation between P3 and P4 mineralisation intervals in different individuals. While Price et al. (2017) focused mainly on mandibular elements, the Lubná dataset focused mostly on maxillary teeth, providing a potential explanation for the different mineralisation intervals identified in the two datasets. We therefore highlight mandibular/maxillary specific mineralisation patterns as an avenue for future research.

### Seasonal mobility of the Lubná reindeer

The Lubná reindeer  $^{87}\text{Sr}/^{86}\text{Sr}$  profiles vary over a notably smaller isotopic range than that documented among the geologies of Central Europe (Fig. 3b). This significantly restricts the range of possible movements made by the reindeer as their teeth were forming. In particular, the absence of enamel  $^{87}\text{Sr}/^{86}\text{Sr}$  ratios above 0.7118 rules out the possibility that any Lubná reindeer spent significant time on the loess beds of SE Germany (which range between  $\sim 0.712$ – $0.715$ ). This likely indicates that the wider North European

Plains region can also be ruled out, as the topographic barriers formed by the Ore, Krkonoše and Orlické Mountains would have channelled fauna migrating between Bohemia and SE Germany across these loess beds, thus imparting a more radiogenic  $^{87}\text{Sr}/^{86}\text{Sr}$  signal. It can also be definitively stated that none of the Lubná reindeer spent significant time in the higher-altitude areas of the Bohemian-Moravian highlands lying to the southeast of Lubná, or the Pilsen and Carlsbad highlands to the west and south, which are predicted to generate  $^{87}\text{Sr}/^{86}\text{Sr}$  values of 0.712 or higher.

Instead, the Lubná reindeer  $^{87}\text{Sr}/^{86}\text{Sr}$  profiles coincide almost exactly with the ranges defined for the loess-covered foothills of the Bohemian-Moravian highlands around Prague, and for the flat expanse of the Bohemian basin, centred on the river Elbe and extending northwest up to the Czech-German border. The foothills near Lubná sit between 200 and 500 m above present sea level and are characterised by at times pronounced hills and valleys, which rise progressively towards the south and east approaching the Bohemian-Moravian highlands (Fig. 1). These foothills would have made ideal habitat for reindeer, characterised by seasonally varied altitude-based gradients in temperature and plant foods. Similarly, the open plains of the Bohemian basin would have provided a classic mammoth steppe habitat in the Late Gravettian, well suited to supporting reindeer herds competing with other species for food.

The available basemap data suggest that the Bohemian basin and the foothills region partially overlap in strontium isoscape terms, but can be distinguished at the upper and lower ends of their collective range as the Bohemian basin trends towards less radiogenic values while the Bohemian foothills trend towards higher signatures, the latter likely reflecting input of erosion products from nearby more radiogenic geologies (Fig. 3b). At the Czech-German border a plant sample and a water sample from the river Elbe gave  $^{87}\text{Sr}/^{86}\text{Sr}$  values of 0.711091 and 0.711332 respectively, at the upper end of the range identified in the Lubná reindeer (Fig. 3). Located geographically at the margins of the German loess beds, these values plausibly represent a mix of the more radiogenic German loess and less radiogenic deposits in the Bohemian basin. Geologies with middling values are probably reasonably localised in their extent where the two deposits meet.

Based on these observations we suggest that the majority of Lubná reindeer, including individuals 1, 2, 3, 5, 8 and 9 which have  $^{87}\text{Sr}/^{86}\text{Sr}$  profiles substantially overlapping with the dentine-defined local Lubná range, remained in the Bohemian-Moravian foothills for the whole period recorded in the teeth. Specifically, reindeer 1, 2, 9 and teeth grouped as Individual 3 were present here during the summer and autumn seasons, and the peaks observed in their  $^{87}\text{Sr}/^{86}\text{Sr}$  profiles likely reflect visits to more radiogenic parts of these

foothills, perhaps areas of higher ground to the south. The  $^{87}\text{Sr}/^{86}\text{Sr}$  profile for reindeer 5 covers late summer, autumn and winter and shows evidence for two brief movements to an isotopically distinct area in the final 5 mm of tooth growth (Fig. 4). This most likely also represents movement within the foothills region itself, and we note again the ~300 m altitudinal variations between hills and valleys that characterises this landscape, which would have been ideal territory for reindeer moving stochastically in search of food. Finally, reindeer 8 is the only individual to have captured a full winter-summer transition (based on the  $\delta^{18}\text{O}$  curve), indicating mobility within the foothills region over a period of at least six months.

In contrast, reindeer 4, 6 and 7 show the most weakly-radiogenic signatures in the dataset, indicating that they most likely spent several seasons in the Bohemian basin during the tooth mineralisation period. In reindeer 4 and 6 this corresponds to late summer, autumn and early winter of the second year of life. The pattern in reindeer 7 is slightly different, showing clear evidence of movement between the basin and a more radiogenic region indistinguishable from the local Lubná range. We suggest this indicates a pattern of seasonal migration, characterised by springtime movements from the Bohemian basin to the foothills region where the reindeer spent the summer months, with return migrations occurring in either late summer (M1, first year of life) or early winter (after M3 mineralisation had ceased, second year of life). Overall, these data show that during the period of tooth growth reindeer 4, 6 and 7 were all absent from the Lubná region at certain seasons of the year, and thus would have been unavailable to hunt at these times.

A potential alternative interpretation of the radiogenic peaks in  $^{87}\text{Sr}/^{86}\text{Sr}$  of reindeer 1, 2, 3 and 8 could be short-term visits to the Czech-German border region, where matching isoscape  $^{87}\text{Sr}/^{86}\text{Sr}$  ratios are found in the basemap data (Figs. 3 and 4). This seems unlikely, however, as movements into and out of this region from the Bohemian basin would be expected to produce rapid changes between relatively low and rather high  $^{87}\text{Sr}/^{86}\text{Sr}$  ratios, which are not seen in the Lubná reindeer. The reindeer  $^{87}\text{Sr}/^{86}\text{Sr}$  profiles also overlap with basemap ranges assigned to the Orlické mountains (north Bohemian Massif Uplands). However, given the evidence for periodic glaciation of the Bohemian massif at higher altitudes (Růžička 2004), and the fact that other higher altitude areas such as the Bohemian-Moravian highlands were abandoned in the Late Gravettian, we consider it unlikely that the Lubná reindeer visited these areas.

In summary, our combined dataset suggests that the reindeer targeted by Late Gravettian hunters at Lubná lived in herds centred on the foothills of the Bohemian-Moravian highlands and in the flat Bohemian Cretaceous plains, with seasonal migration within or between these two regions

detected in a small number of individuals. The data also suggest that reindeer were available to hunt in the Lubná foothills region in all seasons of the year, with a seasonal influx of additional animals during the spring and summer months that migrated up from the Cretaceous plains.

### Dental Cementum and season of death

Dental cementum in three reindeer showed a final thick, fast-growth band or first signs of a slow growth band that was just starting to become visible (Table 5). Dental cementum in the remaining reindeer was either recrystallised or too badly weathered to confidently assign a season of death based on cementum banding. Reindeer cementum growth is generally fast during the spring, summer and autumn months and slow during the winter months, although the duration of the winter annuli varies between populations (Pike-Tay et al. 1995; Grue and Jensen 1979). The three Lubná reindeer with visible cementum banding therefore all died in the autumn or early winter. These results agree with findings reported from zooarchaeological analyses at Lubná revealing the presence of 3–5 month old reindeer, suggesting an early autumn season of death (Wilczyński et al. 2021). Almost no antler was recovered from the site, contrary to expectations for reindeer that died in the autumn or early winter. This indicates that antler was systematically removed from the site for use elsewhere, or possibly that it was processed in a specific place in an unexcavated part of the site (Wilczyński et al. 2021).

Strontium and oxygen isotope profiles for reindeer 4 and 6 indicate that they were not present in the vicinity of Lubná in the autumn-early winter period in the second year of life. Given the evidence for Lubná being a short-term autumn-winter kill-butcher site, these reindeer must have changed their mobility patterns or perhaps moved entirely into the foothills region in the years after tooth growth was completed in order for them to have become prey for the Late Gravettian hunters at Lubná.

## Discussion

Central European geology is highly varied, creating potential for high-magnitude variability in intra-tooth and intra-individual enamel  $^{87}\text{Sr}/^{86}\text{Sr}$  profiles in mobile reindeer. Our results show that this potential is not in fact reflected in the Lubná reindeer. There is no evidence in our data for long-distance mobility over several hundred kilometres, as is observed in some modern reindeer populations (e.g. Theoret et al. 2022; Joly et al. 2019; Burch 1972). Instead, the Lubná reindeer apparently moved relatively short distances across a rather restricted range of geologies. Our analysis additionally shows that while some reindeer plausibly migrated seasonally between the Cretaceous basin and foothills region, others were relatively sedentary, likely occupying a single territory located in the vicinity of Lubná. This indicates that reindeer were able to locate appropriate food sources locally year-round, probably reflecting the dietary adaptability and mixed feeding practices observed in reindeer elsewhere in the mammoth steppe (Schwartz-Narbonne et al. 2019). Suitable food sources for reindeer should also have existed year-round in the Cretaceous basin, which likely supported a productive mammoth-steppe ecosystem during the Late Gravettian. Explanations for reindeer mobility between the basin and foothills region might include competition with other species for those food sources (e.g. Schwartz-Narbonne et al. 2019), or harassment by parasitic warble flies which are known to push reindeer towards cold or windy places such as snow patches or mountain slopes in efforts to avoid them (Burch 1972: 347). Such places may well have existed in the foothills region during the Late Gravettian and, given Lubná's location, it is interesting that reindeer hunters in more recent times have been observed specifically targeting such locations knowing that their chances of encountering reindeer prey there are greatly increased (Burch 1972: 347).

It is noteworthy that the Lubná reindeer did not visit any higher-altitude locations above ~400–450 m a.s.l., despite their tolerance for cold and their ability to thrive in rugged

**Table 5** Results of dental cementum analysis

Individual	Sample ID	Element	N of sections studied	Cementum condition	Final cementum band	Season of death
2	LB5	LP <sup>3</sup>	1	Minor weathering	Thick summer band	Autumn
	LB8	LP <sup>2</sup>	1	Weathered	Thick summer band	Autumn
8	LB1	RM <sub>3</sub>	1	Minor weathering	Slow growth increment just started	Late autumn / early winter
3	LB10	LP <sup>4</sup>	1	Weathered	Slow growth increment just started	Late autumn / early winter
	LB11	LM <sup>1</sup>	2	Recrystallised	Unreadable	Indeterminate
	LB12	LM <sup>3</sup>	1	Recrystallised	Unreadable	Indeterminate
1	LB3	RM <sub>2</sub>	2	Heavy weathering	Unreadable	Indeterminate
4	LB15	LP <sup>3</sup>	2	Recrystallised	Unreadable	Indeterminate
6	LB18	LP <sup>4</sup>	1	Heavy weathering	Unreadable	Indeterminate
	LB19	LP <sup>3</sup>	1	Heavy weathering	Unreadable	Indeterminate
5	LB17	LP <sup>4</sup>	2	None surviving	--	--



upland environments today (Burch et al. 1972). We interpret this pattern as reflecting an altitude-based ecological threshold above which net primary productivity (NPP) dropped to levels insufficient for supporting visiting reindeer, and likely a range of other mammoth steppe fauna too. This is consistent with an absence of upland archaeological occupation in Bohemia and Central Europe more generally during the Gravettian and Late Gravettian periods following an observable shift in settlement patterns, namely that Aurignacian sites regularly occur at higher altitudes than do Gravettian sites in the same landscape (Šída 2009a; Škrdla 2005). Areas of higher ground defined by the Bohemian-Moravian highlands, Carlsbad Highlands, and the Ore, Krkonoše and Orlické mountains thus apparently formed significant topographic barriers to humans and at least some mammoth steppe fauna in the Gravettian and Late Gravettian, constraining their movements to the lower-lying territories centred around river valley corridors and foothills region where Lubná was located.

### Logistical seasonal mobility in the Late Gravettian

Our results indicate that reindeer prey were reliably available in the foothills region continuously throughout the year. We suggest that the Lubná hunters were aware of this when they planned their visit, and specifically chose to hunt reindeer here in the autumn season as part of an organised, seasonal logistical strategy (*sensu* Binford 1980) that targeted different resources and prey at different times of the year. Reindeer are a key source of food (meat and fat), hides and antler, all of which vary seasonally in quality, abundance and/or availability (West 1997:44–48). This is particularly true for critical subcutaneous and marrow fats, which reach peak abundance in reindeer in early autumn, and reindeer hides used for clothing, which require fur of a suitable length: too short and the clothing will not be warm enough; too long and the clothing will be too heavy, too inflexible and the hair will slip more easily (Stenton 1991). This creates a strong seasonal pressure to hunt reindeer in the autumn if they are to be relied upon for clothing needs. Locations where reindeer could predictably have been found during this season would have been attractive to Late Gravettian hunters.

In contrast to the relative stasis of the reindeer, long distance movement of lithic raw materials found at Lubná indicate the connectivity of Late Gravettian hunters with areas at least 120 km away in the north European plains (Wilczyński et al. 2021). Lithic raw material acquisition from remote sources, coupled with toolkits designed for long range mobility, is a particular characteristic of the Late Gravettian in eastern Central Europe (Lengyel and Chu 2016; Lengyel 2018). This Late Gravettian expansion of

foraging area relative to the preceding Pavlovian occurred at the end of Marine Isotope Stage 3, when the apex of the LGM was approaching. Such range expansion matches theoretical predictions for hunter-gatherers reacting to cooler climates and a dwindling quantity and increased variability of food and other resources vital for survival (Kelly 2013).

Lubná is currently the westernmost known Late Gravettian site, as Germany does not preserve archaeological remains from this period, due either to population hiatus or erosional events (Barbieri et al. 2021). We therefore suggest that the Lubná hunters arrived from the east, and engaged in long-distance movements between the north European Plains and the foothills of the Bohemian-Moravian highlands where Lubná is located, geared with a mobile toolkit. Finally, the new isotopic data rule out the possibility that the lithic procurement pattern results from hunters following individual reindeer herds seasonally across the landscape. Rather, we suggest that hunters visited Lubná because they knew reindeer would be present here with a high degree of certainty, representing a reliable and predictable source of food and hides at a critical season of the year.

### Conclusion

Reindeer (*Rangifer tarandus*) was integral to hunter-gatherer subsistence in the Central European Upper Palaeolithic. The direction and timing of any herd movements would therefore have been vital to the decision-making process of Late Gravettian hunters, including those from Lubná VI. We have shown that the hunters at Lubná targeted reindeer herds that were present year-round in the foothills of the Bohemian-Moravian highlands. The hunters visit to Lubná took place within the broader context of a highly mobile lifestyle, yet this mobility was not forced upon Late Gravettian populations by mobility of their reindeer prey. Rather, the highly mobile lifestyle must have been a consequence of other factors related to food and resource acquisition that required a high degree of seasonal mobility. In this context, the permanent availability of reindeer at a particular location must have been attractive to Late Gravettian hunters, as evidenced by the repeated visits made by hunter's to the same hillside, preserved as the Lubná site cluster.

**Supplementary Information** The online version contains supplementary material available at <https://doi.org/10.1007/s12520-024-02019-z>.

**Acknowledgements** This research was funded by the National Science Center, Poland (grant decision No. 2015/18/E/HS3/00178 awarded to J. Wilczyński) and a University of Exeter internal small research grant to A. Pryor. We thank Megan Wilding at the National Oceanography Centre, University of Southampton and Chris Mitchell at the Environment and Sustainability Institute, University of Exeter for assistance

with mass spectrometry analyses. We also thank Wouter Bonhof for assistance with collagen extractions of the bone samples and helpful discussions over many months concerning the isotopic dataset, Amy Horn for comments on a late draft of this manuscript, three anonymous reviewers whose comments improved this manuscript considerably, and all members of the 2018 excavation team at Lubná VI who recovered the materials included in this research.

**Author contributions** CRediT statement Conceptualisation: JW, AJEP; Methodology: JW, AJEP; Formal analysis and investigation: AJEP, TN, CDS, JAM, MC, BH, JC; Writing - original draft preparation: AJEP, TN; Writing - review and editing: all authors; Visualisation: AJEP; Resources: JAM, MC, BH; Project administration: AJEP; Funding acquisition: JW, AJEP. All authors read and approved the final manuscript.

**Funding** This research was funded by the National Science Center, Poland (grant decision No. 2015/18/E/HS3/00178 awarded to J. Wilczyński) and an internal small research grant to A. Pryor from the University of Exeter. The authors additionally certify: The authors have no relevant financial or non-financial interests to disclose. The authors have no competing interests to declare that are relevant to the content of this article. All authors certify that they have no affiliations with or involvement in any organization or entity with any financial interest or non-financial interest in the subject matter or materials discussed in this manuscript. The authors have no financial or proprietary interests in any material discussed in this article.

**Data availability** The original datasets generated during the current study are available as Excel spreadsheets from the corresponding author on reasonable request.

**Code availability** Not applicable.

## Declarations

**Ethics approval** Not applicable.

**Consent for publication** Not applicable.

**Consent to participate** Not applicable.

**Competing interests** The authors declare no competing interests.

**Open Access** This article is licensed under a Creative Commons Attribution 4.0 International License, which permits use, sharing, adaptation, distribution and reproduction in any medium or format, as long as you give appropriate credit to the original author(s) and the source, provide a link to the Creative Commons licence, and indicate if changes were made. The images or other third party material in this article are included in the article's Creative Commons licence, unless indicated otherwise in a credit line to the material. If material is not included in the article's Creative Commons licence and your intended use is not permitted by statutory regulation or exceeds the permitted use, you will need to obtain permission directly from the copyright holder. To view a copy of this licence, visit <http://creativecommons.org/licenses/by/4.0/>.

## References

Ambrose SH (1990) Preparation and characterization of bone and tooth collagen for isotopic analysis. *J Archaeol Sci* 17(4):431–451

- Ambrose SH (1993) Isotopic analysis of paleodiets: methodological and interpretive considerations. In: Sandford MK (ed) *Investigations of ancient human tissue: chemical analyses in anthropology*. Langhorne, PA, Gordon and Breach Science, pp 59–130
- Ampel L, Bigler C, Wohlfarth B, Risberg J, Lotter AF, Veres D (2010) Modest summer temperature variability during DO cycles in western Europe. *Q Sci Rev* 29(11–12):1322–1327
- Barbieri A, Bachofer F, Schmaltz EM, Leven C, Conard NJ, Miller CE (2021) Interpreting gaps: a geoarchaeological point of view on the Gravettian record of Ach and Lone valleys (Swabian Jura, SW Germany). *J Archaeol Sci* 127:1–13
- Bendl J, Vokurka K, Sundvoll B (1993) Strontium and neodymium isotope study of bohemian basalts. *Mineral Petrol* 48(1):35–45
- Bentley RA (2006) Strontium isotopes from the earth to the archaeological skeleton: a review. *J Archaeol Method Theory* 13(3):135–187
- Bentley RA, Knipper C (2005) Geographical patterns in biologically available strontium, carbon and oxygen isotope signatures in prehistoric SW Germany. *Archaeometry* 47(3):629–644
- Bentley RA, Bickle P, Fibiger L, Nowell GM, Dale CW, Hedges REM, Hamilton J, Wahl J, Francken M, Grupe G, Lenneis E, Teschler-Nicola M, Arbogast R-M, Hofmann D, Whittle A (2012) Community differentiation and kinship among Europe's first farmers. *Proc Natl Acad Sci* 109(24):9326–9330
- Bergerud AT (1970) Eruption of permanent premolars and molars for Newfoundland caribou. *J Wildl Manage* 34(4):962–963
- Bergerud AT (1972) Food habits of Newfoundland caribou. *J Wildl Manage* 36:913–923
- Bergerud AT, Luttich SN (2003) Predation risk and optimal foraging trade-off in the demography and spacing of the George River Herd, 1958 to 1993. *Rangifer Special Issue* 14:169–191
- Bergman CM, Schaefer JA, Luttich SN (2000) Caribou movement as a correlated random walk. *Oecologia* 123:364–374
- Binford LR (1980) Willow smoke and dogs tails - hunter-gatherer settlement systems and archaeological site formation. *Am Antiq* 45(1):4–20
- Bocherens H (2015) Isotopic tracking of large Carnivore palaeoecology in the mammoth steppe. *Q Sci Rev* 117:42–71
- Bocherens H, Drucker DG, Bonjean D, Bridault A, Conard NJ, Cupillard C, Ziegler R (2011) Isotopic evidence for dietary ecology of cave lion (*Panthera spelaea*) in North-Western Europe: Prey choice, competition and implications for extinction. *Quatern Int* 245(2):249–261
- Bocherens H, Drucker DG, Germonpré M, Lázníčková-Galetová M, Naito YI, Wissing C, Brůžek J, Oliva M (2015) Reconstruction of the Gravettian food-web at Předmostí I using multi-isotopic tracking (13 C, 15 N, 34S) of bone collagen. *Quatern Int* 359–360:211–228
- Boertje RD (1984) Seasonal diets of the Denali Caribou Herd, Alaska. *Arctic* 37:161–165
- Böhm J (1933) Diluviální stanice v Lubné u Rakovníka. *Věstník Musejního Spolku královského města Rakovníka*. 23:42–51
- Bouchud J (1966) *Essai sur le Renne et la Climatologie Du Paléolithique Moyen et Supérieur*. Imprimerie Magne, Périgeux
- Bråthen KA, Pugnaire FI, Bardgett RD (2021) The paradox of forbs in grasslands and the legacy of the mammoth steppe. *Front Ecol Environ* 19(10):584–592
- Britton K, Grimes V, Dau J, Richards MP (2009) Reconstructing faunal migrations using intra-tooth sampling and strontium and oxygen isotope analyses: a case study of modern caribou (*Rangifer tarandus Grandi*). *J Archaeol Sci* 36:1163–1172
- Britton K, Grimes V, Niven L, Steele TE, McPherron S, Soressi M, Kelly TE, Jaubert J, Hublin J-J, Richards MP (2011) Strontium isotope evidence for migration in late Pleistocene *Rangifer*: implications for neanderthal hunting strategies at the Middle palaeolithic site of Jonzac, France. *J Hum Evol* 61:176–185

- Britton K, Jimenez E-L, Le Corre M, Pederzani S, Daujeard C, Jaouen K, Moncel M-H (2023) Multi-isotope zooarchaeological investigations at Abri Du Maras: the paleoecological and paleoenvironmental context of neanderthal subsistence strategies in the Rhône Valley during MIS 3. *J Hum Evol* 174:103292
- Brown WAB, Chapman NG (1991a) The dentition of red deer (*Cervus elaphus*): a scoring scheme to assess age from wear of the permanent molariform teeth. *J Zool Lond* 224:519–536
- Brown WAB, Chapman NG (1991b) Age assessment of fallow deer (*Dama dama*): from a scoring scheme based on radiographs of developing permanent molariform teeth. *J Zool Lond* 224:367–379
- Brugère A, Fontana L (2009) Mammoth origin and exploitation patterns at Milovice (area G excepted). In: Oliva M (ed) *Milovice: site of the mammoth people below the Pavlov hills*. Moravské Zemské Muzeum, Brno, pp 53–105
- Burch ES Jr. (1972) The Caribou/Wild Reindeer as a human resource. *Am Antiq* 37(3):339–368
- Clark PU, Dyke AS, Shakun JD, Carlson AE, Clark J, Wohlfarth B, Mitrovica JX, Hostetler SW, McCabe AM (2009) The last glacial Maximum. *Science* 325(5941):710–714
- Coplen TB, Kendall C, Hoppo J (1983) Comparison of stable isotope reference samples. *Nature* 302(5905):236–238
- Craine JM, Elmore AJ, Wang L, Augusto L, Baisden WT, Brookshire ENJ, Cramer MD, Hasselquist NJ, Hobbie EA, Kahmen A, Koba K, Kranabetter JM, Mack MC, Marin-Spiotta E, Mayor JR, McLauchlan KK, Michelsen A, Nardoto GB, Oliveira RS, Perakis SS, Peri PL, Quesada CA, Richter A, Schipper LA, Stevenson BA, Turner BL, Viani RA, Wanek G, W. and, Zeller B (2015) Convergence of soil nitrogen isotopes across global climate gradients. *Sci Rep* 5(1):8280
- Davis WL (1986) *Oral histology*. W.B. Saunders, Philadelphia, PA
- de Jong HN (2013) A Strontium Isotope Perspective on Subsistence Through Intra-tooth and Inter-site Variation by LA-MC-ICP-MS and TIMS. Ph. D. thesis. University of Bristol
- de Jong HN, Foster GL, Hawkesworth C, Pike AWG (2007) LA-MC-ICPMS 87Sr/86Sr on tooth enamel - pitfalls and problems. *Geochim Cosmochim Acta* 71:A212
- DeNiro MJ (1985) Postmortem preservation and alteration of in vivo bone collagen isotope ratios in relation to paleodietary reconstruction. *Nature* 317:806–809
- Denton GH, Alley RB, Comer GC, Broecker WS (2005) The role of seasonality in abrupt climate change. *Q Sci Rev* 24(10–11):1159–1182
- Drucker D, Bocherens H, Pike-Tay A, Mariotti A (2001) Isotopic tracking of seasonal dietary change in dentine collagen: preliminary data from modern caribou. *Earth Planet Sci* 333(5):303–309
- Drucker D, Bocherens H, Billiou D (2003) Evidence for shifting environmental conditions in Southwestern France from 33,000 to 15,000 years ago derived from carbon-13 and nitrogen-15 natural abundances in collagen of large herbivores. *Earth Planet Sci Lett* 216(1–2):163–173
- Drucker DG, Kind CJ, Stephan E (2011) Chronological and ecological information on late-glacial and early Holocene reindeer from northwest Europe using radiocarbon ( $^{14}\text{C}$ ) and stable isotope ( $^{13}\text{C}$ ,  $^{15}\text{N}$ ) analysis of bone collagen: case study in southwestern Germany. *Quatern Int* 245(2):218–224
- Drucker DG, Bridault A, Cupillard C (2012) Environmental context of the Magdalenian settlement in the Jura Mountains using stable isotope tracking ( $^{13}\text{C}$ ,  $^{15}\text{N}$ ,  $^{34}\text{S}$ ) of bone collagen from reindeer (*Rangifer tarandus*). *Quatern Int* 272–273:322–332
- Drucker DG, Vercoutère C, Chiotti L, Nespoulet R, Crépin L, Conard NJ, Münzel SC, Higham T, van der Plicht J, Lázničková-Galetová M, Bocherens H (2015) Tracking possible decline of woolly mammoth during the Gravettian in Dordogne (France) and the Ach Valley (Germany) using multi-isotope tracking ( $^{13}\text{C}$ ,  $^{14}\text{C}$ ,  $^{15}\text{N}$ ,  $^{34}\text{S}$ ,  $^{18}\text{O}$ ). *Quatern Int* 359–360:304–317
- Erbán Kochergina YV, Novak M, Erban V, Stepanova M (2021) 87Sr/86Sr isotope ratios in trees as an archaeological tracer: limitations of linking plant-biomass and bedrock Sr isotope signatures. *J Archaeol Sci* 133:105438
- Ericson JE (1985) Strontium isotope characterization in the study of prehistoric human ecology. *J Hum Evol* 14(5):503–514
- Farquhar GD, Ehleringer JR, Hubick KT (1989) Carbon isotope discrimination and photosynthesis. *Annu Rev Plant Physiol Plant Mol Biol* 40:503–537
- Faure G (1986) *Principles of isotope geology*. Wiley, New York
- Ferguson SH, Elkie PC (2004) Seasonal movement patterns of woodland caribou (*Rangifer tarandus caribou*). *J Zool* 262:125–134
- Fiala J, Henjes-Kunst F, Müller-Sigmund H, Vejnar Z (2014) Litho-geochemistry and Sr-Nd isotopic composition of neoproterozoic metasedimentary rocks of the Tepla Crystalline Complex, western Bohemian Massif: a geotectonic interpretation. *J Geosci* 59(4):293–311
- Garrett S, Bogle G, Adams D, Egelberg J (1981) The effect of notching into dentin on new cementum formation during periodontal wound healing. *J Periodontol Res* 16:358–361
- Gerling C (2015) Prehistoric mobility and Diet in the West Eurasian Steppes 3500 to 300 BC. An Isotopic Approach. De Gruyter, Berlin
- Gerling C, Lewis J (2017) High resolution husbandry: the application of 87Sr/86Sr measurements by LA-MC-ICPMS as an approach to tracking prehistoric faunal mobility. In: Scharl S, Gehlen B (eds) *Mobility in prehistoric sedentary societies*. Papers of the CRC 806 workshop in Cologne 26–27 June 2015. Verlag Marie Leidorf GmbH, Rahden/Westf., pp 163–179
- Gigleux C, Grimes V, Tütken T, Knecht R, Britton K (2019) Reconstructing caribou seasonal biogeography in little ice age (late Holocene) Western Alaska using intra-tooth strontium and oxygen isotope analysis. *J Archaeol Science: Rep* 23:1043–1054
- Green DR, Smith TM, Green GM, Bidlack FB, Tafforeau P, Colman AS (2018) Quantitative reconstruction of seasonality from stable isotopes in teeth. *Geochim Cosmochim Acta* 235:483–504
- Grue H, Jensen B (1979) Review of the formation of incremental lines in tooth cementum of terrestrial mammals. *Dan Rev Game Biol* 11(3):3–48
- Guthrie RD (2001) Origin and causes of the mammoth steppe: a story of cloud cover, woolly mammal tooth pits, buckles, and inside-out Beringia. *Q Sci Rev* 20(1–3):549–574
- Hoppe KA, Koch PL, Furutani TT (2003) Assessing the preservation of biogenic strontium in fossil bones and tooth enamel. *Int J Osteoarchaeology* 13(1–2):20–28
- Iacumin P, Bocherens H, Mariotti A, Longinelli A (1996) Oxygen isotope analyses of co-existing carbonate and phosphate in biogenic apatite: a way to monitor diagenetic alteration of bone phosphate? *Earth Planet Sci Lett* 142(1–2):1–6
- Joly K, Gurarie E, Sorum MS, Kaczynsky P, Cameron MD, Jakes AF, Borg BL, Nandintsetseg D, Hopcraft JGC, Buuveibaatar B, Jones PF, Mueller T, Walzer C, Olson KA, Payne JC, Yadamtsuren A, Hebblewhite M (2019) Longest terrestrial migrations and movements around the world. *Sci Rep* 9(1):15333
- Jones SJ (1981) *Dental tissues*. In: Osborne JW (ed) *Dental anatomy and Embryology*. Blackwell, Oxford, pp 66–209
- Kelly RL (2013) *The lifeways of hunter-gatherers: the foraging spectrum*. Cambridge University Press, Cambridge
- Kušta J (1891a) Památky práce lidské v útvarech diluvialních v Čechách. *Věstník Královské české společnosti nauk 1890, II. pololetí, třída matematicko - přírodovědecká* 14: 231–239, tab. X, XI
- Kušta J (1891b) Stanice diluvialního člověka u Lubné v Čechách. *Rozpravy České akademie věd a umění* 1, II. třída, 9: 1–6 (169–172)

- Lazzerini N, Balter V, Coulon A, Tacaïl T, Marchina C, Lemoine M, Bayarkhuu N, Turbat T, Lepetz S, Zazzo A (2021) Monthly mobility inferred from isoscapes and laser ablation strontium isotope ratios in caprine tooth enamel. *Sci Rep* 11(1):2277
- Lee-Thorp JA (2008) On isotopes and old bones. *Archaeometry* 50(6):925–950
- Lengyel G (2018) Lithic analysis of the Middle and Late Upper Palaeolithic in Hungary. *Folia Quaternaria* 86:5–157
- Lengyel G, Chu W (2016) Long thin blade production and late gravettian hunter-gatherer mobility in Eastern Central Europe. *Quatern Int* 406/A:166–173
- Lengyel G, Wilczyński J (2018) The Gravettian and the Epigravettian chronology in eastern central Europe: a comment on Bösken et al. (2017). *Palaeogeogr Palaeoclimatol Palaeoecol* 506:265–269
- Lewis J, Coath CD, Pike AWG (2014) An improved protocol for  $^{87}\text{Sr}/^{86}\text{Sr}$  by laser ablation multi-collector inductively coupled plasma mass spectrometry using oxide reduction and a customised plasma interface. *Chem Geol* 390:173–181
- Lieberman DE (1994) The Biological basis for Seasonal increments in Dental Cementum and their application to Archaeological Research. *J Archaeol Sci* 21(4):525–539
- Lieberman DE, Meadow RH (1992) The biology of cementum increments (an archaeological perspective). *Mammal Rev* 22:57–77
- Lindgren A, Hugelius G, Kuhry P, Christensen TR, Vandenberghe J (2016) GIS-based maps and Area estimates of Northern Hemisphere Permafrost Extent during the last glacial Maximum. *Permafrost Periglacial Process* 27(1):6–16
- Lipecki G, Wojtal P (1998) Mammal remains. In J. K. Kozłowski (Ed.), *Complex of Upper Palaeolithic Sites near Moravany, Western Slovakia. Vol. 2 Moravany-Lopata (Excavations 1993–1996)* (pp. 103–126): Institute of Archaeology, Jagellonian University, Cracow / Archaeological Institute, Slovak Academy of Sciences, Nitra
- Longin R (1971) New Method of collagen extraction for Radiocarbon Dating. *Nature* 230(5291):241–242
- Longinelli A, Iacumin P, Davanzo S, Nikolaev V (2003) Modern reindeer and mice: revised phosphate-water isotope equations. *Earth Planet Sci Lett* 214(3–4):491–498
- Lugli F, Cipriani A, Arnaud J, Arzarello M, Peretto C, Benazzi S (2017) Suspected limited mobility of a Middle Pleistocene woman from Southern Italy: strontium isotopes of a human deciduous tooth. *Sci Rep* 7(1):8615
- Lugli F, Cipriani A, Capocchi G, Ricci S, Boschini F, Boscato P, Iacumin P, Badino F, Mannino MA, Talamo S, Richards MP, Benazzi S, Ronchitelli A (2019) Strontium and stable isotope evidence of human mobility strategies across the last glacial Maximum in southern Italy. *Nat Ecol Evol* 3(6):905–911
- Martin C, Bentaleb I, Kaandorp R, Iacumin P, Chatri K (2008) Intra-tooth study of modern rhinoceros enamel  $\delta^{18}\text{O}$ : is the difference between phosphate and carbonate  $\delta^{18}\text{O}$  a sound diagenetic test? *Palaeogeogr Palaeoclimatol Palaeoecol* 266(3):183–189
- McArthur JM, Howarth RJ, Shields GA (2012) Strontium isotope stratigraphy. In: Gradstein FM, Ogg JG, Schmitz MD, Ogg GM (eds) *The geologic time scale*. Elsevier B.V., Boston, pp 127–144
- Miller FL (1974) Biology of the Kaminuriak population of barren-ground caribou part 2: dentition as an indicator of sex and age; com-position and socialization of the population. *Can Wildl Service Rep Ser* 31:1–88
- Möller P, Dulski P, Gerstenberger H, Morteani G, Fuganti A (1998) Rare earth elements, yttrium and H, O, C, Sr, Nd and Pb isotope studies in mineral waters and corresponding rocks from NW-Bohemia, Czech Republic. *Appl Geochem* 13(8):975–994
- Morris PA (1972) A review of mammalian age determination methods. *Mammal Rev* 2:69–104
- Musil R (2010) Palaeoenvironment at Gravettian sites in Central Europe with emphasis on Moravia (Czech Republic). *Quartär* 57:95–123
- Parker GR (1972) Biology of the Kaminuriak population of barren-ground caribou. Part I. Total numbers, mortality, recruitment, and seasonal distribution. *Canadian Wildlife Service Report Series* 20
- Pasda K (2009) Osteometry, and osteological age and sex determination of the Sisimut reindeer population (*Rangifer tarandus groenlandicus*). *British Archaeological reports International Series* (Vol. 1947). John and Erica Hedges Ltd, Oxford
- Passey BH, Cerling TE, Schuster GT, Robinson TF, Roeder BL, Krueger SK (2005) Inverse methods for estimating primary input signals from time-averaged isotope profiles. *Geochim Cosmochim Acta* 69(16):4101–4116
- Pederzani S, Britton K (2019) Oxygen isotopes in bioarchaeology: principles and applications, challenges and opportunities. *Earth Sci Rev* 188:77–107
- Pederzani S, Aldeias V, Dibble HL, Goldberg P, Hublin J-J, Madelaine S, McPherron SP, Sandgathe D, Steele TE, Turq A, Britton K (2021a) Reconstructing late pleistocene paleoclimate at the scale of human behavior: an example from the neanderthal occupation of La Ferrassie (France). *Sci Rep* 11(1):1419
- Pederzani S, Britton K, Aldeias V, Bourgon N, Fewlass H, Lauer T, McPherron Shannon P, Rezek Z, Sirakov N, Smith Geoff M, Spasov R, Tran NH, Tsanova T, Hublin J-J (2021b) Subarctic climate for the earliest Homo sapiens in Europe. *Sci Adv* 7(39):eabi4642
- Pellegrini M, Snoeck C (2016) Comparing bioapatite carbonate pretreatments for isotopic measurements: part 2 - impact on carbon and oxygen isotope compositions. *Chem Geol* 420:88–96
- Pellegrini M, Lee-Thorp JA, Donahue RE (2011) Exploring the variation of the  $\delta^{18}\text{O}_\text{p}$  and  $\delta^{18}\text{O}_\text{c}$  relationship in enamel increments. *Palaeogeogr Palaeoclimatol Palaeoecol* 310(1–2):71–83
- Pike-Tay A (1995) Variability and synchrony of seasonal indicators in dental cementum microstructure of the Kaminuriak *Rangifer* population. *Archaeofauna* 4:273–284
- Pike-Tay A, Cabrera Valdés V, Bernaldo de Quirós F (1999) Seasonal variations of the Middle-Upper Paleolithic transition at El Castillo, Cueva Morín and El Pendo (Cantabria, Spain). *J Hum Evol* 36(3):283–231
- Piskorska T, Stefaniak K, Krajcarz M, Krajcarz MT (2015) Reindeer during the Upper Palaeolithic in Poland: aspects of variability and paleoecology. *Quatern Int* 359–360:157–177
- Price TD, Knipper C, Grupe G, Smrcka V (2004) Strontium isotopes and prehistoric Human Migration: the Bell Beaker Period in Central Europe. *Eur J Archaeol* 7(1):9–40
- Price TD, Meiggs D, Weber M-J, Pike-Tay A (2017) The migration of late pleistocene reindeer: isotopic evidence from northern Europe. *Archaeol Anthropol Sci* 9:371–394
- Prichard AK, Finstad GL, Shain DH (1999) Lactation in yearling alaskan reindeer: implications for growth, reproduction, and survival. *Rangifer* 19:77–84
- Pryor AJE (2008) Following the fat: food and mobility in the European Upper Palaeolithic 45,000 to 18,000 BP. *Archaeol Rev Camb* 23(2):161–179
- Pryor AJE, Stevens RE, O'Connell TC, Lister JR (2014) Quantification and propagation of errors when converting vertebrate biomineral oxygen isotope data to temperature for palaeoclimate reconstruction. *Palaeogeogr Palaeoclimatol Palaeoecol* 412:99–107
- Pryor AJE, Insoll T, Evis L (2020a) Laser ablation strontium isotope analysis of human remains from Harlaa and Sofi, eastern Ethiopia, and the implications for Islamisation and mobility. *STAR: Science & Technology of Archaeological Research* 6(1): 113–136
- Pryor AJE, Pospuła S, Nesnídalová T, Kowalik N, Wojtal P, Wilczyński J (2020b) Mobility and season of death of the Arctic foxes killed by Gravettian hunters at Kraków Spadzista, Poland. *J Archaeol Science: Rep* 33:102520

- Rabanus-Wallace MT, Wooller MJ, Zazula GD, Shute E, Jahren AH, Kosintsev P, Burns JA, Breen J, Llamas B, Cooper A (2017) Megafaunal isotopes reveal role of increased moisture on rangeland during late pleistocene extinctions. *Nat Ecol Evol* 1(5):0125
- Reade H, Tripp JA, Charlton S, Grimm SB, Leesch D, Müller W, Stevens RE (2020) Deglacial landscapes and the late Upper Palaeolithic of Switzerland. *Q Sci Rev* 239:106372
- Reade H, Grimm SB, Tripp JA, Neruda P, Nerudová Z, Roblíčková M, Sayle KL, Kearney R, Brown S, Douka K, Higham TFG, Stevens RE (2021) Magdalenian and Epimagdalenian chronology and palaeoenvironments at Kůlna Cave, Moravia, Czech Republic. *Archaeol Anthropol Sci* 13(1):4
- Rees JW, Kainer RA, Davis RW (1966) Chronology of mineralization and eruption of mandibular teeth in mule deer. *J Wildl Manage* 30(3):629–631
- Rivals F, Mihlbachler MC, Solounias N, Mol D, Semperebon GM, de Vos J, Kalthoff DC (2010) Palaeoecology of the mammoth steppe fauna from the late Pleistocene of the North Sea and Alaska: separating species preferences from geographic influence in paleoecological dental wear analysis. *Palaeogeogr Palaeoclimatol Palaeoecol* 286(1):42–54
- Rivals F, Drucker DG, Weber M-J, Audouze F, Enloe JG (2020) Dietary traits and habitats of the reindeer (*Rangifer tarandus*) during the late glacial of Northern Europe. *Archaeol Anthropol Sci* 12(5):98
- Rousseau D-D, Chauvel C, Sima A, Hatte C, Lagroix F, Antoine P, Balkanski Y, Fuchs M, Mellett C, Kageyama M, Ramstein G, Lang A (2014) European glacial dust deposits: geochemical constraints on atmospheric dust cycle modeling. *Geophys Res Lett* 41:7666–7674
- Russell WA, Papanastassiou DA, Tombrello TA (1978) Ca isotope fractionation on the Earth and other solar system materials. *Geochim Cosmochim Acta* 42:1075–1090
- Růžička M (2004) The pleistocene glaciation of Czechia. *Developments Quaternary Sci* 2:27–34
- Schaefer JAC, Bergman CM, Luttich SN (2000) Site fidelity of female caribou at multiple spatial scales. *Landscape Ecol* 15:731–739
- Scheeres M, Knipper C, Hauschild M, Schönfelder M, Siebel W, Pare C, Alt KW (2014) Celtic migrations: fact or fiction? Strontium and oxygen isotope analysis of the Czech cemeteries of Radovesice and Kutná Hora in Bohemia. *Am J Phys Anthropol* 155(4):496–512
- Schwartz-Narbonne R, Longstaffe FJ, Kardynal KJ, Druckenmiller P, Hobson KA, Jass CN, Metcalfe JZ, Zazula G (2019) Reframing the mammoth steppe: insights from analysis of isotopic niches. *Q Sci Rev* 215:1–21
- Selvig KA (1963) Electron microscopy of Hertwig's epithelial sheath and of early dentin and cementum formation in the mouse incisor. *Acta Odontol Scand* 21:175–186
- Šída P (2009a) Rakovník Region. In: Šída P (ed) *The Gravettian of Bohemia. The Dolní Věstonice studies 17*. Academy of Sciences of the Czech Republic, Institute of Archaeology at Brno, Brno
- Šída P (2009b) Nová paleolitická stanice v Lubné (okr. Rakovník). *Archeologie ve středních Čechách* 13(1):85–89
- Šída P (2016) Gravettian lithics assemblages from Lubná (Bohemia). *Quatern Int* 406:120–128
- Skoog RO (1968) Ecology of the caribou (*Rangifer tarandus granti*) in Alaska. Doctoral Thesis. University of California, Berkeley
- Škrdla P (ed) (2005) *The Upper Paleolithic on the middle Course of the Morava River. Dolní Věstonice studies 13*. Academy of Sciences of the Czech Republic, Institute of Archaeology at Brno: Brno
- Škrdla P, Nejman L, Bartík J, Rychtaříková T (2015) Human occupation of Central Europe during the Last Glacial Maximum: new evidence from Moravia, Czech Republic. *Antiquity, Project Gallery* 89(347)
- Škrdla P, Rychtaříková T, Bartík J, Nejman L, Demidenko YE (2018) Last glacial maximum paved stone structures from Mohelno-Plevovce. *Moravia Quartär* 65:51–61
- Speth JD, Spielmann KA (1983) Energy-source, protein-metabolism, and hunter gatherer subsistence strategies. *J Anthropol Archaeol* 2(1):1–31
- Sponheimer M, Lee-Thorp JA (1999) Oxygen isotopes in Enamel Carbonate and their ecological significance. *J Archaeol Sci* 26(6):723–728
- Stenton DR (1991) The adaptive significance of caribou winter clothing for arctic hunter-gatherers. *Études/Inuit/Studies* 15(1):3–28
- Stevens RE, Reade H (2021) Stable isotopes confirm the Banwell Bone Cave Mammal Assemblage Zone represents an MIS 5 fauna. *Quatern Res* 101:245–255
- Stevens RE, Jacobi R, Street M, Germonpré M, Conard NJ, Münzel SC, Hedges REM (2008) Nitrogen isotope analyses of reindeer (*Rangifer tarandus*), 45,000 BP to 9,000 BP: palaeoenvironmental reconstructions. *Palaeogeogr Palaeoclimatol Palaeoecol* 262(1–2):32–45
- Theoret J, Cavedon M, Hegel T, Hervieux D, Schwantje H, Steenweg R, Watters M, Musiani M (2022) Seasonal movements in caribou ecotypes of Western Canada. *Mov Ecol* 10(1):12
- Thirlwall MF (1991) Long-term reproducibility of Multicollector Sr and Nd isotope ratio analysis. *Chem Geology: Isotope Geoscience Sect.* 94(2):85–104
- Uno KT, Fisher DC, Wittemyer G, Douglas-Hamilton I, Carpenter N, Omondi P, Cerling TE (2020) Forward and inverse methods for extracting climate and diet information from stable isotope profiles in proboscidean molars. *Quatern Int* 557:92–109
- van den Berg M, Loonen MJJ, Çakırlar C (2021) Judging a reindeer by its teeth: a user-friendly tooth wear and eruption pattern recording scheme to estimate age-at-death in reindeer (*Rangifer tarandus*). *Int J Osteoarchaeology* 31:417–428
- Vencl S (1966) La station paléolithique de Lubná près de Rakovník (Bohême). In: Filip, J. (Ed.) *Investigations archéologiques en Tchécoslovaquie, Praha*, pp. 25–26
- Verpoorte A (2004) Eastern Central Europe during the Pleniglacial. *Antiquity* 78(300):257–266
- Voerkelius S, Lorenz GD, Rummel S, Quézel CR, Heiss G, Baxter M, Brach-Papa C, Deters-Itzelsberger P, Hoelzl S, Hoogewerff J, Ponzevera E, Van Bocxstaele M, Ueckermann H (2010) Strontium isotopic signatures of natural mineral waters, the reference to a simple geological map and its potential for authentication of food. *Food Chem* 118(4):933–940
- Wada E, Ando T, Kumazawa K (1995) Biodiversity of stable isotope ratios. In: Wada E, Yoneyama T, Minagawa M, Ando T, Fry BD (eds) *Stable isotopes in the Biosphere*. Kyoto University, Japan, pp 7–16
- West DL (1997) Hunting strategies in central Europe during the last glacial maximum. *British Archaeological Reports*, Oxford
- Wilczyński J, Wojtal P, Sobczyk K (2012) Spatial organization of the Gravettian mammoth hunters' site at Kraków Spadzista (southern Poland). *J Archaeol Sci* 39(12):3627–3642
- Wilczyński J, Wojtal P, Łanczont M, Mroczek P, Sobieraj D, Fedorowicz S (2015) Loess, flints and bones: multidisciplinary research at Jaksice II Gravettian site (southern Poland). *Quatern Int*, 359–360, 114–130
- Wilczyński J, Goslar T, Wojtal P, Oliva M, Göhlich UB, Antl-Weiser W, Šída P, Verpoorte A, Lengyel G (2020) New Radiocarbon dates for the late Gravettian in Eastern Central Europe. *Radiocarbon* 62(1):243–259
- Wilczyński J, Šída P, Kufel-Diakowska B, Mroczek P, Pryor A, Oberer T, Sobieraj D, Lengyel G (2021) Population mobility and lithic tool diversity in the late Gravettian - the case study of Lubná VI (Bohemian Massif). *Quatern Int* 587–588:103–126

- Willmes M, Kinsley L, Moncel MH, Armstrong RA, Aubert M, Eggin S, Grün R (2016) Improvement of laser ablation in situ micro-analysis to identify diagenetic alteration and measure strontium isotope ratios in fossil human teeth. *J Archaeol Sci* 70:102–116
- Woodhead J, Swearer S, Hergt J, Maas R (2005) In situ Sr-isotope analysis of carbonates by LA-MC-ICP-MS: interference corrections, high spatial resolution and an example from otolith studies. *J Anal at Spectrom* 20(1):22–27
- Wright LE, Schwarcz HP (1998) Stable carbon and oxygen isotopes in human tooth enamel: identifying breastfeeding and weaning in prehistory. *American Journal of Physical Anthropology*, 106(1), 1–18.
- Zazzo A, Bendrey R, Vella D, Moloney AP, Monahan FJ, Schmidt O (2012) A refined sampling strategy for intra-tooth stable isotope analysis of mammalian enamel. *Geochimica et Cosmochimica Acta* 84:1–13

**Publisher's Note** Springer Nature remains neutral with regard to jurisdictional claims in published maps and institutional affiliations.